Co-activation of selective nicotinic acetylcholine receptor subtypes is required to reverse hippocampal network dysfunction and prevent fear memory loss in Alzheimer's disease

Rahmi Lee, Gayeon Kim, Seonil Kim

Department of Biomedical Sciences, Colorado State University, Fort Collins, CO 80523, USA

*Corresponding author: Seonil Kim

Email: seonil.kim@colostate.edu

Abstract

Alzheimer's disease (AD) is the most common form of dementia with no known cause and cure. Research suggests that a reduction of GABAergic inhibitory interneurons' activity in the hippocampus by beta-amyloid peptide (Aβ) is a crucial trigger for cognitive impairment in AD via hyperexcitability. Therefore, enhancing hippocampal inhibition is thought to be protective against AD. However, hippocampal inhibitory cells are highly diverse, and these distinct interneuron subtypes differentially regulate hippocampal inhibitory circuits and cognitive processes. Moreover, Aβ unlikely affects all subtypes of inhibitory interneurons in the hippocampus equally. Hence, identifying the affected interneuron subtypes in AD to enhance hippocampal inhibition optimally is conceptually and practically challenging. We have previously found that Aβ selectively binds to two of the three major hippocampal nicotinic acetylcholine receptor (nAChR) subtypes, α7- and α4β2-nAChRs, but not α3β4-nAChRs, and inhibits these two receptors in cultured hippocampal inhibitory interneurons to decrease their activity, leading to hyperexcitation and synaptic dysfunction in excitatory neurons. We have also revealed that co-activation of α7- and α4β2-nAChRs is required to reverse the Aβ-induced adverse effects in hippocampal excitatory neurons. Here, we discover that α7- and α4β2-nAChRs predominantly control the nicotinic cholinergic signaling and neuronal activity in hippocampal parvalbumin-positive (PV+) and somatostatin-positive (SST+) inhibitory interneurons, respectively. Furthermore, we reveal that co-activation of these receptors is necessary to reverse hippocampal network dysfunction and fear memory loss in the amyloid pathology model mice. We thus suggest that co-activation of PV+ and SST+ cells is a novel strategy to reverse hippocampal dysfunction and cognitive decline in AD.

Introduction

About 5.7 million Americans currently have Alzheimer's disease (AD); that figure is projected to reach 14 million people by 2050[1]. In 2020, the direct costs to American society of caring for those with AD and related dementias are a total of an estimated $305 billion, which makes AD the most expensive disease in America[1]. However, there is no known cause and cure for AD[2]. Therefore, understanding the neural mechanisms of AD pathogenesis is urgently needed for better diagnostic and therapeutic development.

Both preclinical and clinical studies have shown that cortical and hippocampal hyperactivity is found in the early stages of AD[3, 4]. Increased neuronal activity enhances the release of both beta-amyloid peptide (Aβ)[5, 6] and tau[7, 8], which contributes to AD pathology. Additionally, in patients, hyperexcitability is strongly linked to cognitive decline[4, 9-11]. Hyperactivity in the brain is thus most likely a driver of AD pathology and cognitive impairment. Hence, it could be a potential target for both symptomatic and disease-modifying therapies. However, there is still much to learn about hyperexcitability in AD, including the neuronal circuits that are affected in AD, as well as their composite cell types, and the mechanistic link between hyperactivity and cognitive impairment.

Considering AD is a multifactorial disease, it is likely that several factors, rather than a single cause, act in conjunction to cause neuronal hyperexcitability[3]. Importantly, increased neuronal excitability is observed in the vicinity of Aβ plaques[12, 13]. Studies have also shown that neuronal hyperactivity can promote Aβ accumulation in mice[5, 6]. Besides, reducing neuronal excitability decreases Aβ deposition in mice[6, 9]. This suggests that Aβ is a major trigger of hyperexcitability, which in turn initiates a destructive feedback loop for the cells. However, the mechanisms of how Aβ participates in hyperexcitability are still not fully understood. The hippocampal memory system is particularly vulnerable to AD-related cellular pathology[14]. Distinct subtypes of GABAergic inhibitory interneurons differentially regulate hippocampal activity at the cellular, circuit, and network levels[15, 16]. Therefore, maintaining proper inhibition within the hippocampus is essential to ensure normal cognition. Parvalbumin-positive (PV+) and somatostatin-positive (SST+) cells, two major subtypes of inhibitory interneurons in the hippocampus, mainly provide somatic and dendritic inhibition onto pyramidal cells, respectively, to differentially regulate hippocampal network activity and cognitive processes[16]. Aβ is shown to decrease the activity of inhibitory cells to increase excitation in pyramidal cells[17]. This results in hippocampal hyperexcitability and network dysfunction, leading to cognitive decline in AD[3, 17, 18]. This suggests

that the reduction of hippocampal inhibition by Aβ is a crucial trigger for hyperexcitability-induced cognitive impairment in AD. Hence, enhancing hippocampal inhibition is thought to be protective against AD[19]. However, Aβ unlikely affects all subtypes of hippocampal interneurons equally[20-22]. Therefore, identifying the affected interneuron subtypes in AD to enhance hippocampal inhibition optimally is conceptually and technically challenging.

Cholinergic regulation of GABAergic inhibitory network is generally stronger than direct actions on excitatory neurons in the hippocampus since nicotinic acetylcholine receptors (nAChRs) are more densely expressed in inhibitory interneurons than excitatory cells[23-28]. The loss of cholinergic neurons and nAChR expression in the hippocampus is a prominent AD pathology[29-36]. This suggests that cholinergic dysfunction is likely a primary cause for hippocampal inhibition deficits in AD. Although nAChRs are high-affinity targets for Aβ, contradictory results have been reported describing effects of Aβ on nAChRs[37-39]. For example, Aβ appears to bind to nAChRs producing functional inhibitory effects or receptor activation, depending on Aβ concentration, type of preparation (i.e., monomers, soluble oligomers or fibrils), and incubation times[37-39]. Moreover, nearly 30 subtypes of neuronal nAChRs have been reported in the human brain[40-42]. In fact, the U.S. Food and Drug Administration (FDA)-approved current drugs for AD mostly attempt to delay the general breakdown of acetylcholine, which potentially stimulates all types of acetylcholine receptors. Thus, it is not surprising that these non-selective activators suffer from modest efficacy[31, 43, 44]. This suggests, in turn, that distinct nAChR subtypes are differentially affected in AD. Thus, it is challenging to comprehend how Aβ impacts nAChR functions in AD. Furthermore, the important question of how Aβ-induced subtype-specific disruptions in hippocampal interneuron functions are linked to distinct nAChR subtypes remains unanswered.

The three major nAChR subtypes in the hippocampus are composed of α7, α4β2, and α3β4 subunit combinations[40-42]. Importantly, our previous work using Ca^{2+} imaging in cultured hippocampal neurons has shown that Aβ selectively inhibits α7- and α4β2-nAChRs together, but not α3β4-nAChRs, which reduces overall neuronal activity in interneurons, resulting in neuronal hyperexcitation and synaptic dysfunction in excitatory cells[45, 46]. Additionally, our published data using co-immunoprecipitation have shown that Aβ can specifically bind to α7- and α4-containing nAChRs, but not α3-containing receptors[46]. We have also identified two amino acids that are critical for the interaction of Aβ with α7 and α4 subunits, but not the α3 subunit, providing the molecular mechanism underlying the selective interaction of Aβ with specific nAChRs[46]. In line

with these findings, considerable evidence suggests that Aβ is shown to exert subtype-specific inhibition of α7- and/or α4β2-nAChR function without affecting α3β4-nAChRs[37-39, 45, 47-50]. α7 and α4 subtypes are also more significantly reduced in the brains of AD patients compared to α3-type receptors[51]. This supports the idea that Aβ predominantly reduces neuronal activity in inhibitory neurons via selective inhibition of α7- and α4β2-nAChRs, but not α3β4-nAChRs[45]. In fact, we have revealed that co-activation of α7- and α4β2-nAChRs is required to reverse the Aβ-induced adverse effects in hippocampal excitatory and inhibitory cells[45, 46]. Moreover, non-selective stimulation of acetylcholine receptors exacerbates Aβ effects on cultured neurons[45, 46]. In sum, our published works have shown that selective co-activation of α7- and α4β2-nAChRs is required to reverse the Aβ effects on the activity of inhibitory interneurons in AD. Nonetheless, it is still unknown how the Aβ effects on different nAChR subtypes differentially affect inhibitory interneurons to disrupt hippocampal activity at the local circuits and network, resulting in cognitive decline in AD.

Here, we discover that α7-, α4β2-, and α3β4-nAChRs regulate the cholinergic activity mainly in PV+, SST+, and excitatory cells, respectively. We further reveal that hippocampal network activity is disrupted following fear learning in a widely used amyloid pathology mouse model, 5XFAD mice[52]. Most importantly, we show that co-activation of these receptors is necessary to reverse hippocampal network dysfunction and fear memory loss in 5XFAD mice. This suggests that co-activation of PV+ and SST+ cells is a novel strategy to reverse hippocampal network dysfunction and cognitive decline in AD.

Results

Nicotinic cholinergic regulation of cultured hippocampal PV+ and SST+ interneurons is mainly mediated by α7- and α4β2-nAChRs, respectively.

To determine whether nicotinic cholinergic regulation was stronger in GABAergic inhibitory cells than in excitatory neurons, we first compared nicotinic cholinergic activity between excitatory cells (EX) and inhibitory interneurons (IN) using Ca^{2+} imaging with nicotine uncaging in 12-14 days *in vitro* (DIV) cultured mouse hippocampal neurons as neuronal nAChRs are ligand-gated ion channels, and when activated, they induce membrane depolarization and increase somatic Ca^{2+} levels[53, 54]. We found that nicotinic cholinergic activity measured by Ca^{2+} transients in inhibitory interneurons was significantly higher than in excitatory neurons (EX, 1.000 ± 0.879 $\Delta F/F_0$ and IN, 1.575 ± 1.208 $\Delta F/F_0$, $p = 0.0109$) (**Fig. 1a**). This is consistent with the previous reports that cholinergic regulation of inhibitory cells is stronger than excitatory neurons in the hippocampus[23-28].

We next treated 12-14 DIV cultured mouse hippocampal neurons with nAChR subtype-specific antagonists and conducted Ca^{2+} imaging with nicotine uncaging to identify which subtypes of nAChRs played a crucial role in nicotinic cholinergic regulation of hippocampal excitatory and inhibitory cells. In excitatory cells, when compared to controls (CTRL), acute treatment of 3 μM α-Conotoxin AuIB (αCTx), an α3β4-receptor inhibitor, significantly reduced nicotinic cholinergic activity, while 50 nM α-Bungarotoxin (αBTx), an α7-receptor inhibitor, or 1 μM Dihydro-β-erythroidine hydrobromide (DHβE), an α4β2-receptor inhibitor, had no effects (CTRL, 1.000 ± 0.4921 $\Delta F/F_0$, αBTx, 0.870 ± 0.328 $\Delta F/F_0$, $p = 0.8881$, DHβE, 1.042 ± 0.644 $\Delta F/F_0$, and αCTx, $p = 0.9932$, 0.325 ± 0.362 $\Delta F/F_0$, $p = 0.0003$) (**Fig. 1b and Table S1**). Conversely, in inhibitory cells, when compared to controls (CTRL), αBTx or DHβE treatment significantly reduced nicotine-induced activity, but the α3β4 antagonist had no effect (CTRL, 1.000 ± 0.525 $\Delta F/F_0$, αBTx, 0.398 ± 0.290 $\Delta F/F_0$, $p = 0.0025$, DHβE, 0.335 ± 0.300 $\Delta F/F_0$, $p < 0.0001$, and αCTx, 0.871 ± 0.330 $\Delta F/F_0$, $p = 0.7866$) (**Fig. 1c and Table S2**). This data show that α7- and α4β2-nAChRs are mainly responsible for nicotinic cholinergic activity in hippocampal inhibitory cells, while α3β4-nAChRs are important for nicotinic cholinergic activity in hippocampal excitatory cells. These findings are consistent with the previous reports demonstrating that postsynaptic α7- and α4β2-nAChRs are mainly localized on GABAergic interneurons in the hippocampus and mediate nicotine currents[24, 26], while they are expressed in the presynaptic area of excitatory cells[55-59] to regulate neurotransmitter release without neuronal activation such as action potentials. This suggests that stimulation of α7- and α4β2-nAChRs

has more profound effects on neuronal activation in inhibitory cells than excitatory neurons in the hippocampus.

We next analyzed subtype-specific roles of nAChRs in cultured hippocampal PV+ and SST+ interneurons. Since α3β4-nAChRs are shown to mainly regulate excitatory neurons, we focused on the role of α7- and α4β2-nAChRs in these inhibitory cells. In PV+ interneurons, when compared to controls (CTRL), acute treatment of αBTx significantly reduced nicotinic cholinergic activity, while DHβE had no effects (CTRL, 1.000 ± 0.590 $\Delta F/F_0$, αBTx, 0.507 ± 0.374 $\Delta F/F_0$, $p = 0.0006$, and DHβE, 1.076 ± 0.613 $\Delta F/F_0$, $p = 0.9340$) (**Fig. 1d and Table S3**). Importantly, co-treatment of αBTx and DHβE had no additional effect (αBTx + DHβE, 0.607 ± 0.448 $\Delta F/F_0$, $p = 0.0071$) (**Fig. 1d and Table S3**). Conversely, in SST+ interneurons, when compared to controls (CTRL), acute treatment of DHβE significantly reduced nicotinic cholinergic activity, while αBTx had no effects (CTRL, 1.000 ± 0.426 $\Delta F/F_0$, αBTx, 0.917 ± 0.519 $\Delta F/F_0$, $p = 0.8707$, and DHβE, 0.524 ± 0.262 $\Delta F/F_0$, $p < 0.0001$) (**Fig. 1e and Table S4**). Importantly, co-treatment of αBTx and DHβE had no additional effect (αBTx + DHβE, 0.533 ± 0.272 $\Delta F/F_0$, $p < 0.0001$) (**Fig. 1e and Table S4**). This shows that α7- and α4β2-nAChRs play important roles in nicotinic cholinergic regulation of PV+ and SST+ cells, respectively.

The Aβ-induced decrease in the neuronal activity of PV+ and SST+ interneurons is reversed by stimulation of α7- and α4β2-nAChRs, respectively.

We next examined whether Aβ affected nicotinic cholinergic activity of PV+ and SST+ interneurons using nicotine uncaging as described in **Fig. 1**. We found that 250 nM soluble Aβ42 oligomers (oAβ42) treatment significantly reduced nicotine-induced activity in both PV+ (sAβ42, 1.000 ± 0.772 $\Delta F/F_0$ and oAβ42, 0.448 ± 0.233 $\Delta F/F_0$, $p = 0.0038$) and SST+ interneurons (sAβ42, 1.000 ± 0.391 $\Delta F/F_0$ and oAβ42, 0.600 ± 0.237 $\Delta F/F_0$, $p = 0.0002$) compared to neurons treated with 250 nM scrambled Aβ42 (sAβ42) (**Fig. 2a-b**). We further determined how Aβ affected neuronal activity in PV+ and SST+ interneurons. As somatic Ca^{2+} levels in neurons indicate neuronal activity[60], we measured spontaneous somatic Ca^{2+} activity without tetrodotoxin (TTX) in 12-14 DIV cultured hippocampal neurons as carried out previously[45, 46, 61, 62]. 250 nM oAβ42 treatment significantly decreased neuronal activity in both PV+ and SST+ interneurons (PV+ cells; sAβ42, 1.000 ± 0.379 $\Delta F/F_{min}$ and oAβ42, 0.589 ± 0.223 $\Delta F/F_{min}$, $p = 0.0371$, and SST+ cells; sAβ42, 1.000 ± 0.500 $\Delta F/F_{min}$ and

oAβ42, 0.650 ± 0.330 $\Delta F/F_{min}$, p = 0.0206) (**Fig. 2c-d and Table S5-6**). To determine subtype-specific roles of nAChRs in the Aβ effect on PV+ and SST+ cells' activity, we treated these cells with 250 nM oAβ42 or 250 nM sAβ42 and subtype-specific nAChR agonists - 1 μM PNU-282987 (PNU), an α7 agonist, 2 μM RJR-2403 Oxalate (RJR), an α4β2 agonist, or 1 μM NS-3861 (NS), an α3β4 agonist. In PV+ interneurons, when compared to controls (CTRL), activation of α7-nAChRs was sufficient to reverse the Aβ effects, while stimulation of other nAChR subtype had no effects (oAβ42:CTRL, 0.589 ± 0.223 $\Delta F/F_{min}$, oAβ42:PNU, 1.408 ± 0.806 $\Delta F/F_{min}$, p < 0.0001, and oAβ42:RJR, 0.528 ± 0.299 $\Delta F/F_{min}$, p > 0.9999) (**Fig. 2c and Table S5**). In SST+ interneurons, when compared to controls (CTRL), stimulation of α4β2-nAChRs reversed the Aβ effects, but other agonists had no effects (oAβ42:CTRL, 0.650 ± 0.328 $\Delta F/F_{min}$, oAβ42:PNU, p = 0.9900, 0.557 ± 0.271 $\Delta F/F_{min}$, and oAβ42:RJR, 0.994 ± 0.358 $\Delta F/F_{min}$, p = 0.0413) (**Fig. 2d and Table S6**). Activation of α3β4 receptors had no effects on the activity of both PV+ and SST+ interneurons (PV+ Cells; oAβ42:NS, 0.550 ± 0.384 $\Delta F/F_{min}$, p > 0.9999, and SST+ cells; oAβ42:NS, 0.561 ± 0.249 $\Delta F/F_{min}$, p = 0.9946) (**Fig. 2c-d and Table S5-6**), which is consistent with the findings that α3β4-nAChRs are important for nicotinic cholinergic activity in excitatory cells (**Fig. 1b-c**). This suggests that the Aβ-induced decrease in the neuronal activity of PV+ and SST+ interneurons is reversed by stimulation of α7- and α4β2-nAChRs, respectively. This further shows that stimulation of α7- and α4β2-nAChRs is a novel and ideal way to stimulate PV+ and SST+ interneurons' activity rather than excitatory neurons' activity.

Deficits in hippocampal network activity in 5XFAD mice following fear learning.

The hippocampal memory system is particularly vulnerable to AD-related cellular pathologies[14]. Neural network activity in the hippocampus plays important roles in memory processes[63-67]. Studies have shown that altered hippocampal network activity can impair learning and memory processes, which contributes to the development of AD[11, 68-71]. In people at high risk of developing AD, abnormal activation and/or deactivation of specific network activities during hippocampal memory processes are detected decades before the onset of clinical disease[4, 11, 68-71]. This suggests that monitoring hippocampal network activity may be a useful tool for early detection and diagnosis of AD. Hippocampal inhibitory interneurons regulate network oscillations of local field potentials (LFPs), which are thought to play a mechanistic role in various aspects of hippocampus-

dependent memory processes[16, 63-67]. In mice, it has been reported that theta (4-8 Hz) synchrony is increased between the hippocampal CA1 and lateral amygdala during the consolidation and reconsolidation of fear memory[63, 64]. Research also suggests that gamma rhythms (30-100 Hz) are two functionally distinct oscillatory activities, slow (30-50 Hz) and fast (50-100 Hz) gamma[66, 72, 73]. Fast gamma rhythms promote the transmission of current sensory information to the hippocampus during new memory encoding[66, 73]. Slow gamma oscillations are likely involved in storing memory[74-76]. It has been shown that spatial learning increases theta, slow gamma, and fast gamma powers in the hippocampal CA1 area[77-79]. We thus first recorded hippocampal LFPs before and following contextual fear conditioning (CFC) to determine if hippocampal network activity was disrupted in 5XFAD mice after fear learning. Prior to learning, basal LFPs were recorded for an hour (PRE) (**Fig. 3a**). Consolidation of hippocampus-dependent fear memory occurs between 1 and 3 hours after training[80, 81]. Therefore, test animals were returned to their home cage for 90 minutes after fear learning, and then we recorded hippocampal LFPs for additional one hour (POST) (**Fig. 3a**). We then compared hippocampal theta, slow gamma, and fast gamma powers between 5XFAD mice and their wild-type (WT) littermates. We found that theta (Female; WT PRE, 1.000 ± 1.199 and WT POST, 1.696 ± 1.552, $p = 0.0029$, Male; WT PRE, 1.000 ± 1.270 and WT POST, 1.926 ± 2.849, $p = 0.0001$), slow gamma (Female; WT PRE, 1.000 ± 1.223 and WT POST, 1.624 ± 1.420, $p = 0.0031$, Male; WT PRE, 1.000 ± 1.124 and WT POST, 2.049 ± 2.413, $p = 0.0009$), and fast gamma powers (Female; WT PRE, 1.000 ± 1.086 and WT POST, 1.601 ± 1.372, $p = 0.0008$, Male; WT PRE, 1.000 ± 1.051 and WT POST, 2.467 ± 2.486, $p < 0.0001$) were significantly elevated following CFC in WT female and male mice (**Fig. 3e-g**). Conversely, 5XFAD mice showed significant reduction in powers of theta (Female; 5XFAD PRE, 2.195 ± 6.108 and 5XFAD POST, 0.225 ± 0.210, $p = 0.0015$, Male; 5XFAD PRE, 2.225 ± 3.440 and 5XFAD POST, 0.632 ± 1.227, $p < 0.0001$), slow gamma (Female; 5XFAD PRE, 3.145 ± 7.767 and 5XFAD POST, 0.480 ± 0.342, $p = 0.0007$, Male; 5XFAD PRE, 2.136 ± 3.066 and 5XFAD POST, 0.777 ± 1.221, $p = 0.0001$), and fast gamma bands (Female; 5XFAD PRE, 3.059 ± 7.262 and 5XFAD POST, 0.493 ± 0.284, $p = 0.0005$, Male; 5XFAD PRE, 2.086 ± 2.709 and 5XFAD POST, 0.841 ± 1.000, $p < 0.0001$) (**Fig. 3e-g**). Interestingly, we found significant higher basal powers in 5XFAD mice than WT animals in all frequency bands (**Fig. 3e-g**), which is likely related to Aβ-induced early hippocampal hyperexcitation. These findings suggest that the learning-induced increase in hippocampal oscillations is impaired in 5XFAD mice.

In healthy rodents and humans, the hippocampus exhibits prominent gamma oscillations that emerge at specific phases of theta oscillations known as theta-gamma coupling[82]. The strength of theta-gamma coupling in the hippocampus is correlated with the task load of memory in humans[83]. This coupling is impaired in hippocampal slices in AD model mice[84]. Appropriate phase-amplitude coupling (PAC) and entrainment to hippocampal oscillations are thought to be essential for cognition and have been directly linked to memory performance in humans[83, 85, 86]. We thus calculated the mean vector length (MVL) as an entrainment strength. We found that the MVL in both theta-slow gamma and theta-fast gamma was significantly higher following learning than before learning in WT female and male mice (Theta-slow gamma, Female; WT PRE, 0.036 ± 0.027 and WT POST, 0.067 ± 0.044, $p < 0.0001$, Male; WT PRE, 0.041 ± 0.032 and WT POST, 0.069 ± 0.053, $p < 0.0001$. Theta-fast gamma, Female; WT PRE, 0.059 ± 0.087 and WT POST, 0.076 ± 0.070, $p = 0.0004$, Male; WT PRE, 0.036 ± 0.042 and WT POST, 0.061 ± 0.061, $p < 0.0001$) (**Fig. 3h-i**). In contrast, the theta-slow gamma MVL in 5XFAD mice was significantly lower following learning when compared to the basal condition (Female; 5XFAD PRE, 0.055 ± 0.021 and 5XFAD POST, 0.042 ± 0.018, $p < 0.0001$, Male; 5XFAD PRE, 0.066 ± 0.074 and 5XFAD POST, 0.052 ± 0.068, $p = 0.0481$) (**Fig. 3h-i**). Moreover, there was no difference between the 5XFAD animals' theta-fast gamma MVL before and after learning (Female; 5XFAD PRE, 0.028 ± 0.015 and 5XFAD POST, 0.028 ± 0.022, $p = 0.9556$, Male; 5XFAD PRE, 0.045 ± 0.050 and 5XFAD POST, 0.038 ± 0.057, $p = 0.1462$) (**Fig. 3h-i**). This suggests that fear learning strengthens PAC entrainment in WT mice, consistent with the previous report[87]. However, fear leaning is unable to increase theta-gamma coupling in 5XFAD mice. These findings thus show deficits in hippocampal network activity in 5XFAD mice following fear learning.

Co-activation of α7- and α4β2-nAChRs is required to restore normal hippocampal network activity in 5XFAD mice.

We next compared hippocampal oscillatory activity during memory consolidation between WT and 5XFAD mice. When compared to WT mice, 5XFAD mice exhibited a significant decrease in the powers of theta (Female; WT, 1.000 ± 0.915 and 5XFAD, 0.151 ± 0.149, $p < 0.0001$, Male; WT, 1.000 ± 1.479 and 5XFAD, 0.328 ± 0.637, $p < 0.0001$), slow gamma (Female; WT, 1.000 ± 1.874 and 5XFAD, 0.268 ± 10.167, $p = 0.0017$,

Male; WT, 1.000 ± 1.079 and 5XFAD, 0.341 ± 0.494, $p = 0.0012$), and fast gamma bands (Female; WT, 1.000 ± 0.853 and 5XFAD, 0.297 ± 0.162, $p = 0.0027$, Male; WT, 1.000 ± 1.001 and 5XFAD, 0.341 ± 0.405, $p < 0.0001$) (**Fig. 4a-c**). This indicates impaired fear memory processing in 5XFAD mice. Acetylcholine modulates hippocampal oscillations to control memory processes[88-90]. We thus examined if stimulating α7- and α4β2-nAChRs together was required to reverse hippocampal network deficits in 5XFAD mice after fear conditioning. We found that activation of single receptors by themselves using PNU or RJR had no effect on the powers of theta (Female; 5XFAD:PNU, 0.138 ± 0.234, $p = 0.9253$, and 5XFAD:RJR, 0.193 ± 0.347, $p = 0.7671$, Male; 5XFAD:PNU, 0.123 ± 0.137, $p = 0.3112$, and 5XFAD:RJR, 0.090 ± 0.107, $p = 0.2312$), slow gamma (Female; 5XFAD:PNU, 0.305 ± 0.419, $p = 0.8878$, and 5XFAD:RJR, 0.358 ± 0.729, $p = 0.7453$, Male; 5XFAD:PNU, 0.272 ± 0.157, $p = 0.8194$, and 5XFAD:RJR, 0.142 ± 0.122, $p = 0.4959$), and fast gamma bands (Female; 5XFAD:PNU, 0.269 ± 0.392, $p = 0.9128$, and 5XFAD:RJR, 0.267 ± 0.398, $p = 0.9145$, Male; 5XFAD:PNU, 0.263 ± 0.195, $p = 0.7265$, and 5XFAD:RJR, 0.142 ± 0.139, $p = 0.3619$) (**Fig. 4a-c**). This shows that stimulation of either α7- or α4β2-nAChRs is insufficient to improve hippocampal network activity in 5XFAD mice. However, co-stimulation of α7- and α4β2-nAChRs significantly elevated the powers of theta (Female; 5XFAD:PNU+RJR, 0.518 ± 0.834, $p = 0.0011$, Male; 5XFAD:PNU+RJR, 0.684 ± 0.986, $p = 0.0229$), slow gamma (Female; 5XFAD:PNU+RJR, 1.058 ± 1.633, $p = 0.0003$, Male; 5XFAD:PNU+RJR, 1.300 ± 2.375, $p < 0.0001$), and fast gamma bands (Female; 5XFAD:PNU+RJR, 1.253 ± 1.919, $p < 0.0001$, Male; 5XFAD:PNU+RJR, 1.261 ± 1.763, $p < 0.0001$) (**Fig. 4a-c**). These findings suggest a memory consolidation-mediated increase in hippocampal oscillations is disrupted in 5XFAD mice, which is reversed only by co-activation of α7- and α4β2-nAChRs.

We next analyzed the strength of theta-gamma coupling in the hippocampus. We found that the MVL in both theta-slow gamma and theta-fast gamma was significantly lower in 5XFAD mice following learning than WT animals (Theta-slow gamma, Female; WT, 0.067 ± 0.044 and 5XFAD, 0.042 ± 0.018, $p = 0.0004$, Male; WT, 0.070 ± 0.053 and 5XFAD, 0.052 ± 0.068, $p = 0.0202$. Theta-fast gamma, Female; WT, 0.076 ± 0.070 and 5XFAD, 0.028 ± 0.022, $p < 0.0001$, Male; WT, 0.061 ± 0.061 and 5XFAD, 0.038 ± 0.057, $p = 0.0012$) (**Fig. 4d-e**). Interestingly, we found that activation of single receptors or two receptors together was sufficient to increase MVL in 5XFAD mice (Theta-slow gamma, Female; 5XFAD:PNU, 0.072 ± 0.053, $p < 0.0001$,

5XFAD:RJR, 0.100 ± 0.062, $p < 0.0001$, and 5XFAD:PNU+RJR, 0.120 ± 0.040, $p < 0.0001$, Male; 5XFAD:PNU, 0.122 ± 0.054, $p < 0.0001$, 5XFAD:RJR, 0.107 ± 0.032, $p < 0.0001$, and 5XFAD:PNU+RJR, 0.071 ± 0.053, $p < 0.0001$. Theta-fast gamma, Female; 5XFAD:PNU, 0.086 ± 0.036, $p = 0.0004$, 5XFAD:RJR, 0.086 ± 0.036, $p < 0.0001$, and 5XFAD:PNU+RJR, 0.078 ± 0.041, $p < 0.0001$, Male; 5XFAD:PNU, 0.097 ± 0.047, $p < 0.0001$, 5XFAD:RJR, 0.077 ± 0.057, $p = 0.0002$, and 5XFAD:PNU+RJR, 0.056 ± 0.046, $p = 0.0246$) (**Fig. 4d-e**). This shows that activation of α7- and/or α4β2-nAChRs is sufficient to strengthen fear learning consolidation-related PAC entrainment in 5XFAD mice. In sum, 5XFAD mice showed significant deficits in hippocampal network activity following fear conditioning. While stimulation of α7- and/or α4β2-nAChRs is sufficient to increase PAC in 5XFAD mice, co-activation of α7- and α4β2-nAChRs, perhaps stimulating PV+ and SST+ cells together, is essential to restore normal powers of AD-related hippocampal oscillations following fear learning.

Co-activation of α7- and α4β2-nAChRs is required to improve contextual fear memory in 5XFAD mice.

Conditioned fear responses have been demonstrated to be impaired in patients with mild to moderate AD[91, 92]. Fear memory loss in 5XFAD mice starts at the age of 5 months[93]. We thus carried out contextual fear conditioning (CFC) as described previously[94, 95] with 5-month-old 5XFAD and WT female and male mice. In consistent with the previous finding[5], 5XFAD female and male mice intraperitoneally given saline displayed significant less freezing in contextual fear conditioning compared to WT controls, indicating impaired hippocampus-dependent fear memory (Female, WT:Saline, 36.785 ± 10.866% and 5XFAD:Saline, 14.188 ± 12.202%, $p < 0.0001$, and Male, WT:Saline, 38.938 ± 13.066% and 5XFAD:Saline, 16.177 ± 8.761%, $p < 0.0001$) (**Fig. 5**). Given that co-activation of α7- and α4β2-nAChRs is required to reverse fear learning-associated hippocampal network activity (**Fig. 4**), we examined the effects of stimulating these receptors on contextual fear memory in 5XFAD mice (**Fig. 3a**). We intraperitoneally injected PNU or RJR into 5XFAD and WT mice to see if activation of either α7- or α4β2-nAChRs reversed impaired contextual fear memory in AD model mice. Notably, neither PNU nor RJR single injection reversed fear memory loss in 5XFAD mice (Female, 5XFAD:PNU, 15.751 ± 10.332%, $p > 0.9999$, and 5XFAD:RJR, 14.836 ± 10.400%, $p > 0.9999$, and Male, 5XFAD:PNU, 15.558 ± 6.577%, $p > 0.9999$, and 5XFAD:RJR, 14.648 ± 6.018%, $p > 0.9999$) (**Fig. 5**).

This shows that stimulation of either α7- or α4β2-nAChRs is insufficient to improve fear memory in 5XFAD mice. We thus intraperitoneally injected PNU and RJR together into 5XFAD and WT littermates and examined whether co-activation of α7- and α4β2-nAChRs improved contextual fear memory in 5XFAD mice. We found that co-activation of α7- and α4β2-nAChRs significantly enhanced contextual fear memory in 5XFAD male and female mice (Female, 5XFAD:PNU+RJR, 43.664 ± 13.580%, $p < 0.0001$, and Male, 5XFAD:PNU+RJR, 43.434 ± 21.002%, $p = 0.0101$) (**Fig. 5**). Taken all together, we discover that co-activation of α7- and α4β2-nAChRs (potentially stimulates hippocampal PV+ and SST+ cells together) is required to improve hippocampus-dependent fear memory in 5XFAD mice.

Discussion

A large body of research has suggested that Aβ-induced inhibitory dysfunction in the hippocampus can be a crucial trigger for disruptions in neural oscillations and consequent cognitive function in AD[4, 96-102]. However, the molecular mechanisms underlying Aβ-induced hippocampal interneuron dysfunctions in AD have not been studied in depth. Cholinergic dysfunction may be a prime suspect for Aβ-induced inhibitory dysfunction because cholinergic signaling has greater effects on hippocampal inhibitory cells than excitatory neurons[23-28], and there are diverse lines of evidence that molecular interactions between Aβ and nAChRs impair receptor functions in the early stage of AD[54, 103-105]. Aβ thus likely inhibits nAChR activities in inhibitory interneurons, which reduces hippocampal inhibition and oscillations to trigger cognitive decline in the early stage of AD. However, hippocampal inhibitory cells are highly diverse, and distinct interneuron subtypes differentially contributes to hippocampal oscillations and memory formation[16]. In addition, various neuronal nAChRs have been found in the human brain[40-42], and distinct nAChR subtypes differentially affect hippocampal inhibition and oscillations[57, 106-108]. Therefore, it is challenging to elucidate the nAChR-mediated mechanisms by which Aβ affects hippocampal neural network and memory processing in AD at the interneuron subtype levels. Our published works have discovered that Aβ selectively binds to two of the three major hippocampal nAChR subtypes, α7- and α4β2-nAChRs, but not α3β4-nAChRs, and inhibits these two receptors in cultured hippocampal inhibitory interneurons to decrease their activity, leading to hyperexcitation and synaptic dysfunction in excitatory neurons[45, 46]. We have also revealed that co-activation of α7- and α4β2-nAChRs is required to reverse the Aβ-induced adverse effects in hippocampal neurons[45, 46]. In the current study, we further identify that α7-, α4β2-, and α3β4-nAChRs regulate the cholinergic activity mainly in PV+, SST+, and excitatory cells, respectively. Additionally, we discover that co-activation of α7- and α4β2-nAChRs is necessary to reverse hippocampal network dysfunction and prevent fear memory loss in the amyloid pathology model mice. In sum, our study provides the mechanistic link between hippocampal disinhibition-induced hyperexcitability via altered cholinergic activity, network dysfunction, and memory loss in AD.

Based on our findings, we propose the following model. α7-, α4β2-, and α3β4-nAChRs predominantly control the nicotinic cholinergic signaling in PV+ interneurons that provide somatic inhibition, SST+ interneurons that provides dendritic inhibition, and pyramidal excitatory neurons, respectively, in the hippocampus, which is supported by the previous findings[24, 26, 27, 57, 109-117] (**Fig. 6a**). These distinct cholinergic

regulations of inhibitory activity contribute to inhibition onto pyramidal cells, which controls hippocampal network activity and memory processes (**Fig. 6a**). Aβ selectively inhibits α7- and α4β2-nAChRs in PV+ and SST+ cells, respectively, but not α3β4-nAChRs in excitatory neurons, which reduces inhibition to induce hyperexcitability and network dysfunction in the hippocampus, leading to memory loss in AD (**Fig. 6b**). Stimulation of PV+ or SST+ cells by the activation of each nAChR subtype-specific agonists, PNU-282987 (PNU), an α7 agonist, or RJR-2403 Oxalate (RJR), an α4β2 agonist, is insufficient to reverse the adverse effects of Aβ (**Fig. 6c-d**). Therefore, co-stimulation of hippocampal PV+ and SST+ inhibitory interneurons via activation of α7- and α4β2-nAChRs together is required to be protective against AD (**Fig. 6e**).

Given that cholinergic deficiency is associated with AD, strategies aiming to restore normal cholinergic function have been developed as therapeutic drugs for AD, including several acetylcholinesterase inhibitors[118]. Therefore, all cholinergic synapses can be intensified by these drugs. However, some subtypes of nAChRs that may not be affected by Aβ (e.g. α3β4) can also be activated when attempts are made to use such drugs in the treatment of AD, resulting in unexpected side effects. Moreover, acetylcholinesterase inhibitors have been shown to be only partially effective in reversing experimental deficits in hippocampal-dependent memory in rodents[119]. Consistently, we have revealed a non-selective cholinergic agonist exacerbates Aβ effects on hippocampal neurons[45, 46]. Furthermore, overstimulation of the M1 type metabotropic AChRs adversely affect neuronal activity in the prefrontal cortex, related to working memory[120]. Therefore, acetylcholinesterase inhibitors are not very effective in slowing AD progression due to non-selective stimulation of acetylcholine receptors[121, 122]. There are also discrepancies involving the use of nicotine treatment to stimulate nAChRs to alter cognitive function. For example, nicotine agonists have been found to improve performance in a variety of memory tasks in rodents and non-human primate studies[123], while several other studies have failed to find significant enhancement of learning and memory by nicotine treatment[124]. Nonetheless, nAChR agonists have consistently suggested promising approaches in the treatment of AD[125]. However, clinical trials thus far have been challenged by adverse effects or minimal improvement[126]. Additionally, stimulating one type of nAChRs by using a subtype specific agonist enhances cognitive performance, but other studies find no beneficial effect. For instance, selective α7 nAChR agonists have been reported to improve cognition in a variety of animal models[127-129], while another study has found almost no beneficial effect on learning and memory in mice[130]. An α4β2-nAChR agonist alone can improve working memory only in young rats but not older animals[131]. It is thus

not yet clear whether single activation of specific nAChR subtypes provide optimal efficacy in AD[125]. Research also shows that co-activation of α7- and α4β2-nAChRs has substantially greater neuroprotective effects against a ketamine-based model of schizophrenia-like cognitive impairments in rats, when compared to single receptor stimulation[132]. Moreover, pharmacological inhibition of each α7- or α4β2-nAChR subtype has no effect on working memory in nonhuman primates[133]. These studies suggest that proper cholinergic modulation in hippocampal functions requires both α7- and α4β2-nAChRs. Our published works[45, 46] and current study further support this idea. Therefore, the idea that selective co-activation of nAChRs in the hippocampus can reverse Aβ effects on AD pathology is a new concept, which may lead to innovative and novel therapeutic strategies. In fact, several subtype-specific agonists have been developed for clinical trials, but co-activation of nAChRs has not been applied for clinical trials yet[125]. The current work thus suggests that activation of α7- and α4β2-nAChRs as an innovative and selective way to stimulate hippocampal PV+ and SST+ cells in the hippocampal local circuits, which has potentials for a novel therapeutic strategy in AD.

Materials and Methods

Animals

C57Bl6J (Jax 000664), PV-Cre (Jax 017320), SST-Cre (Jax 018973), and 5XFAD (Jax 034840) mice were obtained from Jackson laboratory and bred in the animal facility at Colorado State University (CSU). Animals were housed under a 12:12 hour light/dark cycle. CSU's Institutional Animal Care and Use Committee (IACUC) reviewed and approved the animal care and protocol (3408).

Primary hippocampal neuronal culture

Postnatal day 0 (P0) male and female C57Bl6J, PV-Cre, or SST-Cre pups were used to produce mouse hippocampal neuron cultures as shown previously[61, 134, 135]. Hippocampi were isolated from P0 C57Bl6J mouse brain tissues and digested with 10 U/mL papain (Worthington Biochemical Corp., LK003176). Mouse hippocampal neurons were plated on following poly lysine-coated dishes for glass bottom dishes (500,000 cells) for Ca^{2+} imaging. Neurons were grown in Neurobasal Medium without phenol red (Thermo Fisher Scientific, 12348017) with B27 supplement (Thermo Fisher Scientific, 17504044), 0.5 mM Glutamax (Thermo Fisher Scientific, 35050061), and 1% penicillin/streptomycin (Thermo Fisher Scientific, 15070063). The previous study evaluates maturation, aging, and death of mouse cortical cultured neurons for 60 days *in vitro* (DIV), which demonstrates that synaptogenesis is prominent during the first 15 days and then synaptic markers remained stable through 60 DIV[136]. In particular, the levels of glutamate receptors increase to a maximum by 10-15 DIV and then remain unchanged through 60 DIV. This indicates that 12-14 DIV neurons that we used here are mature cells, and their maturity is likely comparable to that of older neurons. Additionally, neuronal cultures are shown to contain excitatory and inhibitory cells, cholinergic neurons, as well as glia[45, 46, 137].

Reagents

Soluble Aβ42 oligomers (oAβ42) were prepared as previously described[45, 138]. 1 mg of lyophilized human Aβ42 (Anaspec) was dissolved in 1mL of 1,1,1,3,3,3-hexafluoro-2-propanol (HFIP) (Sigma, St. Louis, MO) to prevent aggregation, portioned into 10 µg aliquots, air-dried and stored at -80 °C. For use in experiments, an aliquot was thawed at room temperature, and then dissolved in DMSO and PBS to make a

100 μM solution. The solution was incubated for 16 hours at 4°C and then diluted to a final concentration for use in experiments. Scrambled Aβ42 oligomers (sAβ42) were prepared the same way for controls. The following nAChR antagonists were used in this study: α-Bungarotoxin (αBTx) (Alomone labs)), an α7 antagonist, Dihydro-β-erythroidine hydrobromide (DHβE) (Tocris Bioscience), an α4β2 antagonist, and α-Conotoxin AuIB (Alomone labs), an α3β4 antagonist. The following nAChR agonists were used in this study: PNU-282987 (PNU) (Tocris Bioscience), an α7 agonist, RJR-2403 Oxalate (RJR) (Tocris Bioscience), an α4β2 agonist, and NS-3861 (NS) (Tocris Bioscience), an α3β4 agonist. Tetrodotoxin (TTX) (Abcam) was used to prevent action potential-dependent spontaneous network activity.

GCaMP Ca^{2+} imaging with nicotine uncaging

For Ca^{2+} imaging with nicotine uncaging, a genetically encoded Ca^{2+} indicator, GCaMP, was used. As the majority of cells in hippocampal cultures are excitatory neurons[139], we expressed GCaMP6f (Addgene #40755)[140] under the control of the CMV promoter by transfection for imaging excitatory cells, and GCaMP6f under the control of the GABAergic neuron-specific enhancer of the mouse *Dlx* (mDlx) gene (Addgene #83899)[141] was transfected for imaging inhibitory interneurons as shown previously[45]. Glass-bottom dishes were mounted on a temperature-controlled stage on an Olympus IX73 microscope and maintained at 37°C and 5% CO_2 using a Tokai-Hit heating stage and digital temperature and humidity controller. For nicotine uncaging, 1 μM photoactivatable nicotine (PA-Nic) (Tocris Bioscience) was added to the culture media, and epi-illumination photolysis (390 nm, 0.12 mW/mm^2, 1 sec) was used as shown previously[53]. TTX (1 μM) was added in culture media to prevent action potential-dependent spontaneous network activity. A baseline average (F_0) of 20 frames (50 ms exposure) were captured in the soma prior to nicotine uncaging, and 50 more frames (50 ms exposure) were obtained after photostimulation. The fractional change in fluorescence intensity relative to baseline ($\Delta F/F_0$) was calculated. For **Fig. 1a**, the average peak amplitude in excitatory cells (EX) was used to normalize the peak amplitude in each cell and was compared to the inhibitory cells' average (IN). For **Fig. 1b-c**, the images were captured right after each antagonist was added to the media. The average peak amplitude in the control group without drug treatment (CTRL) was used to normalize the peak amplitude in each cell, and the control group's average peak amplitude was compared to the experimental groups' average. For **Fig. 1d-e**, PV-Cre and SST-Cre mice were used to culture hippocampal neurons. We infected 4

DIV neurons prepared from PV-Cre or SST-Cre mice with adeno-associated virus (AAV) expressing Cre-dependent GCaMP7s (Addgene# 104495-AAV1) - pGP-AAV-CAG-FLEX-jGCaMP7s-WPRE was a gift from Douglas Kim & GENIE Project (Addgene plasmid #104495 ; http://n2t.net/addgene:104495 ; RRID:Addgene_104495)[142] to determine nicotinic cholinergic activity in PV+ and SST+ cells using nicotine uncaging. For GCaMP7s, the images were captured right after each antagonist was added to the media. A baseline average (F_0) of 20 frames (5 ms exposure) were captured prior to nicotine uncaging, and 100 more frames (5 ms exposure) were obtained after photolysis. The average peak amplitude in the control group (CTRL) was used to normalize the peak amplitude in each cell, and the control group's average peak amplitude was compared to the experimental groups' average. For Fig. 2, PV-Cre and SST-Cre mice were also used to culture hippocampal neurons. For **Fig 2a-b**, Ca^{2+} imaging with nicotine uncaging was conducted as described in **Fig. 1d-e**. The images were captured right after 250 nM sAβ42 or 250 nM oAβ42 was added to the media. The average peak amplitude in sAβ42-treated cells was used to normalize the peak amplitude in each cell, and the sAβ42 group's average peak amplitude was compared to the oAβ42-treated cells' average.

GCaMP Ca^{2+} imaging

We measured spontaneous Ca^{2+} activity in cultured hippocampal excitatory neurons because It has been shown that networks of neurons in culture can produce spontaneous synchronized activity[143]. In fact, network activity emerges at 3-7 DIV independent of either ongoing excitatory or inhibitory synaptic activity and matures over the following several weeks in cultures[143]. Therefore, the somatic Ca^{2+} signals we observed are from the spontaneous network activity in cultured cells. To do this, we used AAV to express Cre-dependent GCaMP7s (Addgene# 104495-AAV1)[142] in cells prepared from PV-Cre or SST-Cre mice. We then measured Ca^{2+} activity in the soma of 14 DIV cultured hippocampal excitatory neurons with a modification of the previously described method[45, 46, 61, 62, 144-146]. For GCaMP7s, the images were captured right after 250 nM sAβ42 or 250 nM oAβ42 was added to the media in the presence or absence of each agonist. A 10 ms exposure time and a total of 100 images were obtained with a one-second interval. F_{min} was determined as the minimum fluorescence value during the imaging. Total Ca^{2+} activity was obtained by 100 values of $\Delta F/F_{min} = (F_t - F_{min}) / F_{min}$ in each image, and values of $\Delta F/F_{min} < 0.1$ were rejected due to potential photobleaching. The average total Ca^{2+} activity in the control group (CTRL) was used to normalize total Ca^{2+} activity in each cell.

The control group's average total Ca^{2+} activity was compared to the experimental groups' average as described previously[45, 46, 61, 144-146].

In vivo activation of nAChRs

For *in vivo* activation of nAChRs, we used PNU-282987 (PNU), an α7-nAChR agonist, and RJR-2403 Oxalate (RJR), an α4β2-nAChR agonist. These agonists have a number of advantages that can be used to test our hypothesis; 1) they are blood-brain barrier (BBB) permeable[129-131, 147, 148], 2) they do not require endogenous acetylcholine to stimulate receptors since they are direct agonists rather than positive allosteric modulators[129, 130, 147, 149-152], and 3) repeated injection of these agonists is sufficient to show receptor activation in the rodent brains without causing receptor desensitization[150, 151, 153-155]. PNU and RJR were prepared at concentrations of 1 mg/ml and intraperitoneally injected into 5-month-old 5XFAD and WT female and male mice at a dose of 5 mg/kg by themselves or together once per day for 7 days, a condition that is sufficient to stimulate each nAChR subtype *in vivo*[129-131, 147]. Saline was given to mice as a control.

Contextual fear conditioning (CFC)

Contextual fear conditioning (Habitest Modular System, Coulbourn Instrument) was carried out as described previously[94, 95]. In Day 1 (encoding), the test mouse was placed in a novel rectangular chamber with a grid floor. After a 3-min baseline period, the test animal was given one shock (a 2 sec, 0.5 mA shock) and stayed in the chamber for an additional 1 min after the shock before being returned to the home cage for overnight (consolidation). A contextual memory test was conducted the next day (Day 2 - retrieval) in the same conditioning chamber for 3 min. Fear memory was determined by measuring the percentage of the freezing response (immobility excluding respiration and heartbeat) using an automated tracking program (FreezeFrame).

Stereotaxic surgery

5-month-old mice were anaesthetized with an intraperitoneal injection of a mixture of ketamine (100 mg/kg) and xylazine (10 mg/kg) and placed in a stereotactic frame. The target craniotomy site for local field potential (LFP) recordings was marked on the skull, and electrodes were implanted bilaterally into the dorsal

hippocampal CA1 area (Bregma coordinates: AP: −1.95 mm, ML: ± 1.12 mm, DV: −1.20 mm). One small screw for the ground anchored at the anterior edges of the surgical site and a wire for a reference in the posterior part of the craniotomy site were bound with dental cement (GC America) to secure the implant in place. The electrodes were constructed by twisting 16 Formvar-insulated NiCh wires (75 μm, California Fine Wire) and attached to a Mill-Max connector. After surgery, mice were treated with antibiotics and analgesic drugs daily, and their health was closely monitored as described in our approved IACUC protocol.

Hippocampal LFP recording

We conducted contextual fear conditioning one week after the surgery as a learning and memory paradigm. Basal LFPs were recorded before learning for one hour (**Fig. 3a**). According to a large body of studies, consolidation of hippocampus-dependent fear memory occurs between 1 and 3 hours after training[80, 81]. Therefore, after fear learning, test animals were returned to their home cage for 90 minutes, and then we recorded hippocampal LFPs for one hour, a time for fear memory consolidation (**Fig. 3a**). LFP data were collected through electrodes which connect to a 16-channel head-stage (Intan Technologies) that digitizes the raw analog LFP signals via an onboard analog-to-digital converter. We used the Open Ephys Acquisition Board[156] to acquire the digitized signal at 2 kHz. The electrode locations were verified histologically at the end of recordings (**Fig. 3b**). If the electrode was placed outside the CA1 area, the animal was excluded in analysis.

LFP data analysis

LFP data were analyzed in MATLAB (The Mathworks Inc.). The data were formatted for importation into the Brainstorm platform[157]. Recorded traces were downsampled to 2 kHz and then bandpass filtered between 0.1 and 200 Hz (**Fig. 3c**). We applied a notch filter at 60 Hz to reduce powerline artifacts. Awake animals' movement may produce more and stronger artifacts in the recorded data[158]. We thus used Independent Component Analysis (ICA) to remove these artifacts. Power spectral density was calculated by a Fast Fourier Transform (FFT) algorithm (**Fig. 3d**). The mean absolute power spectra of the theta (4-8 Hz), slow gamma (30-50 Hz), and fast gamma (50-100 Hz) bands were calculated using Welch's method in the Brainstorm platform[157]. The power of each frequency band was normalized to WT and first compared before and after fear conditioning in WT and 5XFAD mice. We also compared them between WT and 5XFAD mice during memory

consolidation. For theta-gamma phase amplitude coupling (PAC) analysis, we measured the high-frequency bands modulated by theta bands in epochs with a matched, filtered LFP amplitude envelope. Data were filtered into theta, slow gamma, and fast gamma using a phase-invariant, 2nd order Butterworth characteristic filter (MATLAB function filtfilt.m). The analytic signal for each was computed using the Hilbert Transform (MATLAB function hilbert.m), resulting in instantaneous theta phase and gamma band amplitude. The peaks of the gamma-band amplitudes were defined as local maxima at or exceeding the mean + 1 standard deviation (SD) of the baseline gamma-band amplitude from the Hilbert Transform envelopes. The instantaneous theta phase for each peak was extracted. The mean vector length (MVL) was calculated as an entrainment strength. The MVL in each condition was normalized to WT and then compared before and after fear conditioning in WT and 5XFAD mice. We also compared them between WT and 5XFAD mice following fear learning.

Statistical analysis

The Franklin A. Graybill Statistical Laboratory at CSU was consulted for statistical analysis in the current study, including sample size determination, randomization, experiment conception and design, data analysis, and interpretation. We used the GraphPad Prism 10 software to determine statistical significance (set at $p < 0.05$). Grouped results of single comparisons were tested for normality with the Shapiro-Wilk normality or Kolmogorov-Smirnov test and analyzed using an unpaired or paired two-tailed Student's t-test when data are normally distributed. Differences between multiple groups were assessed by N-way analysis of variance (ANOVA) with the Tukey test or Two-stage linear step-up procedure of Benjamini, Krieger and Yekutieli. The graphs were presented as mean ± Standard Deviation (SD).

Acknowledgments

We thank members of the Kim laboratory for their generous support. We appreciate Dr. Eunhye Park for the technical guidance and Dr. Don Rojas to support data analysis. This work is supported by the NIH/NCATS Colorado CTSA Grant (UL1 TR002535), the Boettcher Foundation's Webb-Waring Biomedical Research Program, BrightFocus Foundation, and the NIH grant (1R03AG072102).

References

1. Wong W. Economic burden of Alzheimer disease and managed care considerations. Am J Manag Care. 2020;26(8 Suppl):S177-S83. Epub 2020/08/26. doi: 10.37765/ajmc.2020.88482. PubMed PMID: 32840331.

2. Walsh DM, Selkoe DJ. Amyloid beta-protein and beyond: the path forward in Alzheimer's disease. Curr Opin Neurobiol. 2020;61:116-24. Epub 2020/03/21. doi: 10.1016/j.conb.2020.02.003. PubMed PMID: 32197217.

3. Targa Dias Anastacio H, Matosin N, Ooi L. Neuronal hyperexcitability in Alzheimer's disease: what are the drivers behind this aberrant phenotype? Transl Psychiatry. 2022;12(1):257. Epub 2022/06/23. doi: 10.1038/s41398-022-02024-7. PubMed PMID: 35732622; PMCID: PMC9217953.

4. Gallego-Rudolf J, Wiesman AI, Pichet Binette A, Villeneuve S, Baillet S, Group P-AR. Synergistic association of Abeta and tau pathology with cortical neurophysiology and cognitive decline in asymptomatic older adults. Nat Neurosci. 2024. Epub 20240918. doi: 10.1038/s41593-024-01763-8. PubMed PMID: 39294489.

5. Cirrito JR, Yamada KA, Finn MB, Sloviter RS, Bales KR, May PC, Schoepp DD, Paul SM, Mennerick S, Holtzman DM. Synaptic activity regulates interstitial fluid amyloid-beta levels in vivo. Neuron. 2005;48(6):913-22. Epub 2005/12/21. doi: 10.1016/j.neuron.2005.10.028. PubMed PMID: 16364896.

6. Yamamoto K, Tanei ZI, Hashimoto T, Wakabayashi T, Okuno H, Naka Y, Yizhar O, Fenno LE, Fukayama M, Bito H, Cirrito JR, Holtzman DM, Deisseroth K, Iwatsubo T. Chronic optogenetic activation augments abeta pathology in a mouse model of Alzheimer disease. Cell Rep. 2015;11(6):859-65. Epub 2015/05/06. doi: 10.1016/j.celrep.2015.04.017. PubMed PMID: 25937280.

7. Pooler AM, Phillips EC, Lau DH, Noble W, Hanger DP. Physiological release of endogenous tau is stimulated by neuronal activity. EMBO Rep. 2013;14(4):389-94. doi: 10.1038/embor.2013.15. PubMed PMID: 23412472; PMCID: PMC3615658.

8. Wu JW, Hussaini SA, Bastille IM, Rodriguez GA, Mrejeru A, Rilett K, Sanders DW, Cook C, Fu H, Boonen RA, Herman M, Nahmani E, Emrani S, Figueroa YH, Diamond MI, Clelland CL, Wray S, Duff KE. Neuronal activity enhances tau propagation and tau pathology in vivo. Nat Neurosci. 2016;19(8):1085-92. doi: 10.1038/nn.4328. PubMed PMID: 27322420; PMCID: PMC4961585.

9. Yuan P, Grutzendler J. Attenuation of beta-Amyloid Deposition and Neurotoxicity by Chemogenetic Modulation of Neural Activity. J Neurosci. 2016;36(2):632-41. Epub 2016/01/14. doi: 10.1523/JNEUROSCI.2531-15.2016. PubMed PMID: 26758850; PMCID: PMC4710779.

10. Vossel KA, Ranasinghe KG, Beagle AJ, Mizuiri D, Honma SM, Dowling AF, Darwish SM, Van Berlo V, Barnes DE, Mantle M, Karydas AM, Coppola G, Roberson ED, Miller BL, Garcia PA, Kirsch HE, Mucke L, Nagarajan SS. Incidence and impact of subclinical epileptiform activity in Alzheimer's disease. Ann Neurol. 2016;80(6):858-70. Epub 2016/10/04. doi: 10.1002/ana.24794. PubMed PMID: 27696483; PMCID: PMC5177487.

11. Mondadori CR, Buchmann A, Mustovic H, Schmidt CF, Boesiger P, Nitsch RM, Hock C, Streffer J, Henke K. Enhanced brain activity may precede the diagnosis of Alzheimer's disease by 30 years. Brain : a journal of neurology. 2006;129(Pt 11):2908-22. Epub 2006/10/03. doi: 10.1093/brain/awl266. PubMed PMID: 17012294.

12. Busche MA, Eichhoff G, Adelsberger H, Abramowski D, Wiederhold KH, Haass C, Staufenbiel M, Konnerth A, Garaschuk O. Clusters of hyperactive neurons near amyloid plaques in a mouse model of Alzheimer's disease. Science. 2008;321(5896):1686-9. doi: 10.1126/science.1162844. PubMed PMID: 18802001.

13. Busche MA, Chen X, Henning HA, Reichwald J, Staufenbiel M, Sakmann B, Konnerth A. Critical role of soluble amyloid-beta for early hippocampal hyperactivity in a mouse model of Alzheimer's disease. Proc Natl Acad Sci U S A. 2012;109(22):8740-5. Epub 2012/05/18. doi: 10.1073/pnas.1206171109. PubMed PMID: 22592800; PMCID: PMC3365221.

14. Hyman BT, Trojanowski JQ. Consensus recommendations for the postmortem diagnosis of Alzheimer disease from the National Institute on Aging and the Reagan Institute Working Group on diagnostic criteria for the neuropathological assessment of Alzheimer disease. J Neuropathol Exp Neurol. 1997;56(10):1095-7. Epub 1997/11/05. doi: 10.1097/00005072-199710000-00002. PubMed PMID: 9329452.

15. Freund TF, Buzsaki G. Interneurons of the hippocampus. Hippocampus. 1996;6(4):347-470. Epub 1996/01/01. doi: 10.1002/(SICI)1098-1063(1996)6:4<347::AID-HIPO1>3.0.CO;2-I. PubMed PMID: 8915675.

16. Pelkey KA, Chittajallu R, Craig MT, Tricoire L, Wester JC, McBain CJ. Hippocampal GABAergic Inhibitory Interneurons. Physiological reviews. 2017;97(4):1619-747. Epub 2017/09/29. doi: 10.1152/physrev.00007.2017. PubMed PMID: 28954853; PMCID: PMC6151493.

17. Palop JJ, Mucke L. Amyloid-beta-induced neuronal dysfunction in Alzheimer's disease: from synapses toward neural networks. Nat Neurosci. 2010;13(7):812-8. Epub 2010/06/29. doi: 10.1038/nn.2583. PubMed PMID: 20581818; PMCID: PMC3072750.

18. Kazim SF, Seo JH, Bianchi R, Larson CS, Sharma A, Wong RKS, Gorbachev KY, Pereira AC. Neuronal Network Excitability in Alzheimer's Disease: The Puzzle of Similar versus Divergent Roles of Amyloid beta and Tau. eNeuro. 2021;8(2). Epub 2021/03/21. doi: 10.1523/ENEURO.0418-20.2020. PubMed PMID: 33741601; PMCID: PMC8174042.

19. Palop JJ, Mucke L. Network abnormalities and interneuron dysfunction in Alzheimer disease. Nat Rev Neurosci. 2016;17(12):777-92. Epub 2016/11/11. doi: 10.1038/nrn.2016.141. PubMed PMID: 27829687.

20. Ren SQ, Yao W, Yan JZ, Jin C, Yin JJ, Yuan J, Yu S, Cheng Z. Amyloid beta causes excitation/inhibition imbalance through dopamine receptor 1-dependent disruption of fast-spiking GABAergic input in anterior cingulate cortex. Sci Rep. 2018;8(1):302. Epub 2018/01/13. doi: 10.1038/s41598-017-18729-5. PubMed PMID: 29321592; PMCID: PMC5762926.

21. Caccavano A, Bozzelli PL, Forcelli PA, Pak DTS, Wu JY, Conant K, Vicini S. Inhibitory Parvalbumin Basket Cell Activity is Selectively Reduced during Hippocampal Sharp Wave Ripples in a Mouse Model of Familial Alzheimer's Disease. J Neurosci. 2020;40(26):5116-36. Epub 2020/05/23. doi: 10.1523/JNEUROSCI.0425-20.2020. PubMed PMID: 32439703; PMCID: PMC7314414.

22. Xu Y, Zhao M, Han Y, Zhang H. GABAergic Inhibitory Interneuron Deficits in Alzheimer's Disease: Implications for Treatment. Front Neurosci. 2020;14:660. Epub 2020/07/28. doi: 10.3389/fnins.2020.00660. PubMed PMID: 32714136; PMCID: PMC7344222.

23. Ji D, Lape R, Dani JA. Timing and location of nicotinic activity enhances or depresses hippocampal synaptic plasticity. Neuron. 2001;31(1):131-41. Epub 2001/08/11. PubMed PMID: 11498056.

24. Frazier CJ, Rollins YD, Breese CR, Leonard S, Freedman R, Dunwiddie TV. Acetylcholine activates an alpha-bungarotoxin-sensitive nicotinic current in rat hippocampal interneurons, but not pyramidal cells. J Neurosci. 1998;18(4):1187-95. Epub 1998/03/14. PubMed PMID: 9454829; PMCID: PMC6792737.

25. Hefft S, Hulo S, Bertrand D, Muller D. Synaptic transmission at nicotinic acetylcholine receptors in rat hippocampal organotypic cultures and slices. The Journal of physiology. 1999;515 (Pt 3):769-76. Epub 1999/03/06. doi: 10.1111/j.1469-7793.1999.769ab.x. PubMed PMID: 10066903; PMCID: PMC2269188.

26. Jones S, Yakel JL. Functional nicotinic ACh receptors on interneurones in the rat hippocampus. The Journal of physiology. 1997;504 (Pt 3):603-10. Epub 1997/12/24. PubMed PMID: 9401968; PMCID: PMC1159964.

27. McQuiston AR, Madison DV. Nicotinic receptor activation excites distinct subtypes of interneurons in the rat hippocampus. J Neurosci. 1999;19(8):2887-96. Epub 1999/04/07. PubMed PMID: 10191306; PMCID: PMC6782295.

28. Ji D, Dani JA. Inhibition and disinhibition of pyramidal neurons by activation of nicotinic receptors on hippocampal interneurons. Journal of neurophysiology. 2000;83(5):2682-90. Epub 2000/05/11. doi: 10.1152/jn.2000.83.5.2682. PubMed PMID: 10805668.

29. Nordberg A. Nicotinic receptor abnormalities of Alzheimer's disease: therapeutic implications. Biological psychiatry. 2001;49(3):200-10. PubMed PMID: 11230871.

30. Kadir A, Almkvist O, Wall A, Langstrom B, Nordberg A. PET imaging of cortical 11C-nicotine binding correlates with the cognitive function of attention in Alzheimer's disease. Psychopharmacology. 2006;188(4):509-20. doi: 10.1007/s00213-006-0447-7. PubMed PMID: 16832659.

31. Ferreira-Vieira TH, Guimaraes IM, Silva FR, Ribeiro FM. Alzheimer's disease: Targeting the Cholinergic System. Current neuropharmacology. 2016;14(1):101-15. PubMed PMID: 26813123; PMCID: PMC4787279.

32. Pensalfini A, Kim S, Subbanna S, Bleiwas C, Goulbourne CN, Stavrides PH, Jiang Y, Lee JH, Darji S, Pawlik M, Huo C, Peddy J, Berg MJ, Smiley JF, Basavarajappa BS, Nixon RA. Endosomal Dysfunction Induced by Directly Overactivating Rab5 Recapitulates Prodromal and Neurodegenerative Features of Alzheimer's Disease. Cell Rep. 2020;33(8):108420. Epub 2020/11/26. doi: 10.1016/j.celrep.2020.108420. PubMed PMID: 33238112; PMCID: PMC7714675.

33. Alam JJ, Nixon RA. Disease-modifying pharmacological approaches to correcting basal forebrain cholinergic neuronal (BFCN) dysfunction and degeneration. Neuropsychopharmacology : official publication of the American College of Neuropsychopharmacology. 2021. Epub 2021/08/15. doi: 10.1038/s41386-021-01135-x. PubMed PMID: 34389810.

34. Jiang Y, Rigoglioso A, Peterhoff CM, Pawlik M, Sato Y, Bleiwas C, Stavrides P, Smiley JF, Ginsberg SD, Mathews PM, Levy E, Nixon RA. Partial BACE1 reduction in a Down syndrome mouse model blocks Alzheimer-related endosomal anomalies and cholinergic neurodegeneration: role of APP-CTF. Neurobiol Aging. 2016;39:90-8. Epub 2016/03/01. doi: 10.1016/j.neurobiolaging.2015.11.013. PubMed PMID: 26923405; PMCID: PMC4773919.

35. Chen Y, Dyakin VV, Branch CA, Ardekani B, Yang D, Guilfoyle DN, Peterson J, Peterhoff C, Ginsberg SD, Cataldo AM, Nixon RA. In vivo MRI identifies cholinergic circuitry deficits in a Down syndrome model. Neurobiol Aging. 2009;30(9):1453-65. Epub 2008/01/09. doi: 10.1016/j.neurobiolaging.2007.11.026. PubMed PMID: 18180075; PMCID: PMC2771203.

36. Ginsberg SD, Mufson EJ, Alldred MJ, Counts SE, Wuu J, Nixon RA, Che S. Upregulation of select rab GTPases in cholinergic basal forebrain neurons in mild cognitive impairment and Alzheimer's disease. J Chem Neuroanat. 2011;42(2):102-10. Epub 2011/06/15. doi: 10.1016/j.jchemneu.2011.05.012. PubMed PMID: 21669283; PMCID: PMC3163754.

37. Liu Q, Kawai H, Berg DK. beta -Amyloid peptide blocks the response of alpha 7-containing nicotinic receptors on hippocampal neurons. Proc Natl Acad Sci U S A. 2001;98(8):4734-9. doi: 10.1073/pnas.081553598. PubMed PMID: 11274373; PMCID: PMC31903.

38. Pettit DL, Shao Z, Yakel JL. beta-Amyloid(1-42) peptide directly modulates nicotinic receptors in the rat hippocampal slice. J Neurosci. 2001;21(1):RC120. PubMed PMID: 11150356.

39. Pym L, Kemp M, Raymond-Delpech V, Buckingham S, Boyd CA, Sattelle D. Subtype-specific actions of beta-amyloid peptides on recombinant human neuronal nicotinic acetylcholine receptors (alpha7, alpha4beta2, alpha3beta4) expressed in Xenopus laevis oocytes. British journal of pharmacology. 2005;146(7):964-71. doi: 10.1038/sj.bjp.0706403. PubMed PMID: 16184187; PMCID: PMC1751230.

40. Albuquerque EX, Pereira EF, Alkondon M, Rogers SW. Mammalian nicotinic acetylcholine receptors: from structure to function. Physiological reviews. 2009;89(1):73-120. doi: 10.1152/physrev.00015.2008. PubMed PMID: 19126755; PMCID: PMC2713585.

41. Lindstrom JM. Nicotinic acetylcholine receptors of muscles and nerves: comparison of their structures, functional roles, and vulnerability to pathology. Annals of the New York Academy of Sciences. 2003;998:41-52. PubMed PMID: 14592862.

42. Clementi F, Fornasari D, Gotti C. Neuronal nicotinic receptors, important new players in brain function. European journal of pharmacology. 2000;393(1-3):3-10. PubMed PMID: 10770992.

43. Thompson S, Lanctot KL, Herrmann N. The benefits and risks associated with cholinesterase inhibitor therapy in Alzheimer's disease. Expert Opin Drug Saf. 2004;3(5):425-40. Epub 2004/09/01. doi: 10.1517/14740338.3.5.425. PubMed PMID: 15335298.

44. Mangialasche F, Solomon A, Winblad B, Mecocci P, Kivipelto M. Alzheimer's disease: clinical trials and drug development. Lancet Neurol. 2010;9(7):702-16. Epub 2010/07/09. doi: 10.1016/S1474-4422(10)70119-8. PubMed PMID: 20610346.

45. Sun JL, Stokoe SA, Roberts JP, Sathler MF, Nip KA, Shou J, Ko K, Tsunoda S, Kim S. Co-activation of selective nicotinic acetylcholine receptors is required to reverse beta amyloid-induced Ca(2+) hyperexcitation. Neurobiol Aging. 2019;84:166-77. Epub 2019/10/20. doi: 10.1016/j.neurobiolaging.2019.09.005. PubMed PMID: 31629115.

46. Roberts JP, Stokoe SA, Sathler MF, Nichols RA, Kim S. Selective co-activation of alpha7- and alpha4beta2-nicotinic acetylcholine receptors reverses beta-amyloid-induced synaptic dysfunction. The Journal of biological chemistry. 2021:100402. Epub 2021/02/12. doi: 10.1016/j.jbc.2021.100402. PubMed PMID: 33571523.

47. Grassi F, Palma E, Tonini R, Amici M, Ballivet M, Eusebi F. Amyloid beta(1-42) peptide alters the gating of human and mouse alpha-bungarotoxin-sensitive nicotinic receptors. The Journal of physiology. 2003;547(Pt 1):147-57. doi: 10.1113/jphysiol.2002.035436. PubMed PMID: 12562926; PMCID: PMC2342606.

48. Wu J, Kuo YP, George AA, Xu L, Hu J, Lukas RJ. beta-Amyloid directly inhibits human alpha4beta2-nicotinic acetylcholine receptors heterologously expressed in human SH-EP1 cells. The Journal of biological chemistry. 2004;279(36):37842-51. Epub 2004/07/06. doi: 10.1074/jbc.M400335200. PubMed PMID: 15234980.

49. Magdesian MH, Nery AA, Martins AH, Juliano MA, Juliano L, Ulrich H, Ferreira ST. Peptide blockers of the inhibition of neuronal nicotinic acetylcholine receptors by amyloid beta. The Journal of biological chemistry. 2005;280(35):31085-90. doi: 10.1074/jbc.M502406200. PubMed PMID: 15987688.

50. Olivero G, Grilli M, Chen J, Preda S, Mura E, Govoni S, Marchi M. Effects of soluble beta-amyloid on the release of neurotransmitters from rat brain synaptosomes. Frontiers in aging neuroscience. 2014;6:166. doi: 10.3389/fnagi.2014.00166. PubMed PMID: 25076904; PMCID: PMC4098032.

51. Guan ZZ, Zhang X, Ravid R, Nordberg A. Decreased protein levels of nicotinic receptor subunits in the hippocampus and temporal cortex of patients with Alzheimer's disease. Journal of neurochemistry. 2000;74(1):237-43. PubMed PMID: 10617125.

52. Oakley H, Cole SL, Logan S, Maus E, Shao P, Craft J, Guillozet-Bongaarts A, Ohno M, Disterhoft J, Van Eldik L, Berry R, Vassar R. Intraneuronal beta-amyloid aggregates, neurodegeneration, and neuron loss in

transgenic mice with five familial Alzheimer's disease mutations: potential factors in amyloid plaque formation. J Neurosci. 2006;26(40):10129-40. Epub 2006/10/06. doi: 10.1523/JNEUROSCI.1202-06.2006. PubMed PMID: 17021169; PMCID: PMC6674618.

53. Banala S, Arvin MC, Bannon NM, Jin XT, Macklin JJ, Wang Y, Peng C, Zhao G, Marshall JJ, Gee KR, Wokosin DL, Kim VJ, McIntosh JM, Contractor A, Lester HA, Kozorovitskiy Y, Drenan RM, Lavis LD. Photoactivatable drugs for nicotinic optopharmacology. Nature methods. 2018;15(5):347-50. Epub 2018/03/27. doi: 10.1038/nmeth.4637. PubMed PMID: 29578537; PMCID: PMC5923430.

54. Jurgensen S, Ferreira ST. Nicotinic receptors, amyloid-beta, and synaptic failure in Alzheimer's disease. J Mol Neurosci. 2010;40(1-2):221-9. doi: 10.1007/s12031-009-9237-0. PubMed PMID: 19690986.

55. Radcliffe KA, Dani JA. Nicotinic stimulation produces multiple forms of increased glutamatergic synaptic transmission. J Neurosci. 1998;18(18):7075-83. Epub 1998/09/16. PubMed PMID: 9736631; PMCID: PMC6793238.

56. Alkondon M, Pereira EF, Eisenberg HM, Albuquerque EX. Choline and selective antagonists identify two subtypes of nicotinic acetylcholine receptors that modulate GABA release from CA1 interneurons in rat hippocampal slices. J Neurosci. 1999;19(7):2693-705. Epub 1999/03/23. PubMed PMID: 10087082; PMCID: PMC6786070.

57. Alkondon M, Albuquerque EX. Nicotinic acetylcholine receptor alpha7 and alpha4beta2 subtypes differentially control GABAergic input to CA1 neurons in rat hippocampus. Journal of neurophysiology. 2001;86(6):3043-55. Epub 2001/12/04. doi: 10.1152/jn.2001.86.6.3043. PubMed PMID: 11731559.

58. Maggi L, Sher E, Cherubini E. Regulation of GABA release by nicotinic acetylcholine receptors in the neonatal rat hippocampus. The Journal of physiology. 2001;536(Pt 1):89-100. Epub 2001/10/02. doi: 10.1111/j.1469-7793.2001.00089.x. PubMed PMID: 11579159; PMCID: PMC2278841.

59. Huang LT, Sherwood JL, Sun YJ, Lodge D, Wang Y. Activation of presynaptic alpha7 nicotinic receptors evokes an excitatory response in hippocampal CA3 neurones in anaesthetized rats: an in vivo iontophoretic study. British journal of pharmacology. 2010;159(3):554-65. Epub 2010/01/29. doi: 10.1111/j.1476-5381.2009.00529.x. PubMed PMID: 20105181; PMCID: PMC2828020.

60. Gleichmann M, Mattson MP. Neuronal calcium homeostasis and dysregulation. Antioxid Redox Signal. 2011;14(7):1261-73. doi: 10.1089/ars.2010.3386. PubMed PMID: 20626318; PMCID: PMC3048837.

61. Sztukowski K, Nip K, Ostwald PN, Sathler MF, Sun JL, Shou J, Jorgensen ET, Brown TE, Elder JH, Miller C, Hofmann F, VandeWoude S, Kim S. HIV induces synaptic hyperexcitation via cGMP-dependent protein kinase II activation in the FIV infection model. PLoS biology. 2018;16(7):e2005315. Epub 2018/07/28. doi: 10.1371/journal.pbio.2005315. PubMed PMID: 30052626.

62. Zaytseva A, Bouckova E, Wiles MJ, Wustrau MH, Schmidt IG, Mendez-Vazquez H, Khatri L, Kim S. Ketamine's rapid antidepressant effects are mediated by Ca(2+)-permeable AMPA receptors. Elife. 2023;12. Epub 2023/06/26. doi: 10.7554/eLife.86022. PubMed PMID: 37358072; PMCID: PMC10319435.

63. Seidenbecher T, Laxmi TR, Stork O, Pape HC. Amygdalar and hippocampal theta rhythm synchronization during fear memory retrieval. Science. 2003;301(5634):846-50. Epub 2003/08/09. doi: 10.1126/science.1085818. PubMed PMID: 12907806.

64. Narayanan RT, Seidenbecher T, Sangha S, Stork O, Pape HC. Theta resynchronization during reconsolidation of remote contextual fear memory. Neuroreport. 2007;18(11):1107-11. Epub 2007/06/26. doi: 10.1097/WNR.0b013e3282004992. PubMed PMID: 17589308.

65. Markram H, Lubke J, Frotscher M, Sakmann B. Regulation of synaptic efficacy by coincidence of postsynaptic APs and EPSPs. Science. 1997;275(5297):213-5. Epub 1997/01/10. doi: 10.1126/science.275.5297.213. PubMed PMID: 8985014.

66. Colgin LL. Rhythms of the hippocampal network. Nat Rev Neurosci. 2016;17(4):239-49. Epub 2016/03/11. doi: 10.1038/nrn.2016.21. PubMed PMID: 26961163; PMCID: PMC4890574.

67. Duzel E, Penny WD, Burgess N. Brain oscillations and memory. Curr Opin Neurobiol. 2010;20(2):143-9. Epub 2010/02/26. doi: 10.1016/j.conb.2010.01.004. PubMed PMID: 20181475.

68. Filippini N, MacIntosh BJ, Hough MG, Goodwin GM, Frisoni GB, Smith SM, Matthews PM, Beckmann CF, Mackay CE. Distinct patterns of brain activity in young carriers of the APOE-epsilon4 allele. Proc Natl Acad Sci U S A. 2009;106(17):7209-14. Epub 2009/04/10. doi: 10.1073/pnas.0811879106. PubMed PMID: 19357304; PMCID: PMC2678478.

69. Bateman RJ, Xiong C, Benzinger TL, Fagan AM, Goate A, Fox NC, Marcus DS, Cairns NJ, Xie X, Blazey TM, Holtzman DM, Santacruz A, Buckles V, Oliver A, Moulder K, Aisen PS, Ghetti B, Klunk WE, McDade E, Martins RN, Masters CL, Mayeux R, Ringman JM, Rossor MN, Schofield PR, Sperling RA, Salloway S, Morris JC, Dominantly Inherited Alzheimer N. Clinical and biomarker changes in dominantly inherited Alzheimer's

disease. N Engl J Med. 2012;367(9):795-804. Epub 2012/07/13. doi: 10.1056/NEJMoa1202753. PubMed PMID: 22784036; PMCID: PMC3474597.

70. Reiman EM, Quiroz YT, Fleisher AS, Chen K, Velez-Pardo C, Jimenez-Del-Rio M, Fagan AM, Shah AR, Alvarez S, Arbelaez A, Giraldo M, Acosta-Baena N, Sperling RA, Dickerson B, Stern CE, Tirado V, Munoz C, Reiman RA, Huentelman MJ, Alexander GE, Langbaum JB, Kosik KS, Tariot PN, Lopera F. Brain imaging and fluid biomarker analysis in young adults at genetic risk for autosomal dominant Alzheimer's disease in the presenilin 1 E280A kindred: a case-control study. Lancet Neurol. 2012;11(12):1048-56. Epub 2012/11/10. doi: 10.1016/S1474-4422(12)70228-4. PubMed PMID: 23137948; PMCID: PMC4181671.

71. Herrmann CS, Demiralp T. Human EEG gamma oscillations in neuropsychiatric disorders. Clin Neurophysiol. 2005;116(12):2719-33. Epub 2005/10/29. doi: 10.1016/j.clinph.2005.07.007. PubMed PMID: 16253555.

72. Cobb SR, Buhl EH, Halasy K, Paulsen O, Somogyi P. Synchronization of neuronal activity in hippocampus by individual GABAergic interneurons. Nature. 1995;378(6552):75-8. Epub 1995/11/02. doi: 10.1038/378075a0. PubMed PMID: 7477292.

73. Mably AJ, Colgin LL. Gamma oscillations in cognitive disorders. Curr Opin Neurobiol. 2018;52:182-7. Epub 2018/08/20. doi: 10.1016/j.conb.2018.07.009. PubMed PMID: 30121451; PMCID: PMC6139067.

74. Nakazawa K, Quirk MC, Chitwood RA, Watanabe M, Yeckel MF, Sun LD, Kato A, Carr CA, Johnston D, Wilson MA, Tonegawa S. Requirement for hippocampal CA3 NMDA receptors in associative memory recall. Science. 2002;297(5579):211-8. Epub 2002/06/01. doi: 10.1126/science.1071795. PubMed PMID: 12040087; PMCID: PMC2877140.

75. Steffenach HA, Sloviter RS, Moser EI, Moser MB. Impaired retention of spatial memory after transection of longitudinally oriented axons of hippocampal CA3 pyramidal cells. Proc Natl Acad Sci U S A. 2002;99(5):3194-8. Epub 2002/02/28. doi: 10.1073/pnas.042700999. PubMed PMID: 11867718; PMCID: PMC122495.

76. Treves A, Rolls ET. Computational constraints suggest the need for two distinct input systems to the hippocampal CA3 network. Hippocampus. 1992;2(2):189-99. Epub 1992/04/01. doi: 10.1002/hipo.450020209. PubMed PMID: 1308182.

77. Rossato JI, Gonzalez MC, Radiske A, Apolinario G, Conde-Ocazionez S, Bevilaqua LR, Cammarota M. PKMzeta Inhibition Disrupts Reconsolidation and Erases Object Recognition Memory. J Neurosci.

2019;39(10):1828-41. Epub 2019/01/10. doi: 10.1523/JNEUROSCI.2270-18.2018. PubMed PMID: 30622166; PMCID: PMC6407297.

78. Zheng C, Bieri KW, Hwaun E, Colgin LL. Fast Gamma Rhythms in the Hippocampus Promote Encoding of Novel Object-Place Pairings. eNeuro. 2016;3(2). Epub 2016/06/04. doi: 10.1523/ENEURO.0001-16.2016. PubMed PMID: 27257621; PMCID: PMC4874540.

79. Trimper JB, Stefanescu RA, Manns JR. Recognition memory and theta-gamma interactions in the hippocampus. Hippocampus. 2014;24(3):341-53. Epub 2013/11/15. doi: 10.1002/hipo.22228. PubMed PMID: 24227610; PMCID: PMC4004109.

80. Kwapis JL, Wood MA. Epigenetic mechanisms in fear conditioning: implications for treating post-traumatic stress disorder. Trends Neurosci. 2014;37(12):706-20. Epub 2014/09/16. doi: 10.1016/j.tins.2014.08.005. PubMed PMID: 25220045; PMCID: PMC4258434.

81. Bourtchouladze R, Abel T, Berman N, Gordon R, Lapidus K, Kandel ER. Different training procedures recruit either one or two critical periods for contextual memory consolidation, each of which requires protein synthesis and PKA. Learning & memory. 1998;5(4-5):365-74. Epub 1999/08/24. PubMed PMID: 10454361; PMCID: PMC311273.

82. Nakazono T, Jun H, Blurton-Jones M, Green KN, Igarashi KM. Gamma oscillations in the entorhinal-hippocampal circuit underlying memory and dementia. Neurosci Res. 2018;129:40-6. Epub 2018/02/14. doi: 10.1016/j.neures.2018.02.002. PubMed PMID: 29438778; PMCID: PMC7059556.

83. Axmacher N, Henseler MM, Jensen O, Weinreich I, Elger CE, Fell J. Cross-frequency coupling supports multi-item working memory in the human hippocampus. Proc Natl Acad Sci U S A. 2010;107(7):3228-33. Epub 2010/02/06. doi: 10.1073/pnas.0911531107. PubMed PMID: 20133762; PMCID: PMC2840289.

84. Goutagny R, Gu N, Cavanagh C, Jackson J, Chabot JG, Quirion R, Krantic S, Williams S. Alterations in hippocampal network oscillations and theta-gamma coupling arise before Abeta overproduction in a mouse model of Alzheimer's disease. The European journal of neuroscience. 2013;37(12):1896-902. Epub 2013/06/19. doi: 10.1111/ejn.12233. PubMed PMID: 23773058.

85. Daume J, Kaminski J, Schjetnan AGP, Salimpour Y, Khan U, Kyzar M, Reed CM, Anderson WS, Valiante TA, Mamelak AN, Rutishauser U. Control of working memory by phase-amplitude coupling of human

hippocampal neurons. Nature. 2024;629(8011):393-401. Epub 20240417. doi: 10.1038/s41586-024-07309-z. PubMed PMID: 38632400; PMCID: PMC11078732.

86. Lega B, Burke J, Jacobs J, Kahana MJ. Slow-Theta-to-Gamma Phase-Amplitude Coupling in Human Hippocampus Supports the Formation of New Episodic Memories. Cereb Cortex. 2016;26(1):268-78. Epub 20141014. doi: 10.1093/cercor/bhu232. PubMed PMID: 25316340; PMCID: PMC4677977.

87. Radiske A, Gonzalez MC, Conde-Ocazionez S, Rossato JI, Kohler CA, Cammarota M. Cross-Frequency Phase-Amplitude Coupling between Hippocampal Theta and Gamma Oscillations during Recall Destabilizes Memory and Renders It Susceptible to Reconsolidation Disruption. J Neurosci. 2020;40(33):6398-408. Epub 20200713. doi: 10.1523/JNEUROSCI.0259-20.2020. PubMed PMID: 32661022; PMCID: PMC7424867.

88. Wilson MA, Fadel JR. Cholinergic regulation of fear learning and extinction. Journal of neuroscience research. 2017;95(3):836-52. Epub 2016/10/06. doi: 10.1002/jnr.23840. PubMed PMID: 27704595; PMCID: PMC5241223.

89. Haam J, Yakel JL. Cholinergic modulation of the hippocampal region and memory function. Journal of neurochemistry. 2017;142 Suppl 2:111-21. Epub 2017/08/10. doi: 10.1111/jnc.14052. PubMed PMID: 28791706; PMCID: PMC5645066.

90. Headley DB, Pare D. Common oscillatory mechanisms across multiple memory systems. NPJ Sci Learn. 2017;2. Epub 2017/01/01. doi: 10.1038/s41539-016-0001-2. PubMed PMID: 30294452; PMCID: PMC6171763.

91. Hamann S, Monarch ES, Goldstein FC. Impaired fear conditioning in Alzheimer's disease. Neuropsychologia. 2002;40(8):1187-95. Epub 2002/04/05. doi: 10.1016/s0028-3932(01)00223-8. PubMed PMID: 11931922.

92. Hoefer M, Allison SC, Schauer GF, Neuhaus JM, Hall J, Dang JN, Weiner MW, Miller BL, Rosen HJ. Fear conditioning in frontotemporal lobar degeneration and Alzheimer's disease. Brain : a journal of neurology. 2008;131(Pt 6):1646-57. Epub 2008/05/22. doi: 10.1093/brain/awn082. PubMed PMID: 18492729; PMCID: PMC2544622.

93. Kimura R, Ohno M. Impairments in remote memory stabilization precede hippocampal synaptic and cognitive failures in 5XFAD Alzheimer mouse model. Neurobiology of disease. 2009;33(2):229-35. Epub 2008/11/26. doi: 10.1016/j.nbd.2008.10.006. PubMed PMID: 19026746; PMCID: PMC2741400.

94. Kim S, Pick JE, Abera S, Khatri L, Ferreira DD, Sathler MF, Morison SL, Hofmann F, Ziff EB. Brain region-specific effects of cGMP-dependent kinase II knockout on AMPA receptor trafficking and animal behavior. Learning & memory. 2016;23(8):435-41. doi: 10.1101/lm.042960.116. PubMed PMID: 27421896; PMCID: PMC4947234.

95. Shou J, Tran A, Snyder N, Bleem E, Kim S. Distinct Roles of GluA2-lacking AMPA Receptor Expression in Dopamine D1 or D2 Receptor Neurons in Animal Behavior. Neuroscience. 2018;398:102-12. doi: 10.1016/j.neuroscience.2018.12.002. PubMed PMID: 30537522.

96. Verret L, Mann EO, Hang GB, Barth AM, Cobos I, Ho K, Devidze N, Masliah E, Kreitzer AC, Mody I, Mucke L, Palop JJ. Inhibitory interneuron deficit links altered network activity and cognitive dysfunction in Alzheimer model. Cell. 2012;149(3):708-21. doi: 10.1016/j.cell.2012.02.046. PubMed PMID: 22541439; PMCID: PMC3375906.

97. Park K, Lee J, Jang HJ, Richards BA, Kohl MM, Kwag J. Optogenetic activation of parvalbumin and somatostatin interneurons selectively restores theta-nested gamma oscillations and oscillation-induced spike timing-dependent long-term potentiation impaired by amyloid beta oligomers. BMC Biol. 2020;18(1):7. Epub 2020/01/16. doi: 10.1186/s12915-019-0732-7. PubMed PMID: 31937327; PMCID: PMC6961381.

98. Iaccarino HF, Singer AC, Martorell AJ, Rudenko A, Gao F, Gillingham TZ, Mathys H, Seo J, Kritskiy O, Abdurrob F, Adaikkan C, Canter RG, Rueda R, Brown EN, Boyden ES, Tsai LH. Gamma frequency entrainment attenuates amyloid load and modifies microglia. Nature. 2016;540(7632):230-5. Epub 2016/12/09. doi: 10.1038/nature20587. PubMed PMID: 27929004; PMCID: PMC5656389.

99. Chung H, Park K, Jang HJ, Kohl MM, Kwag J. Dissociation of somatostatin and parvalbumin interneurons circuit dysfunctions underlying hippocampal theta and gamma oscillations impaired by amyloid beta oligomers in vivo. Brain structure & function. 2020;225(3):935-54. Epub 2020/02/29. doi: 10.1007/s00429-020-02044-3. PubMed PMID: 32107637; PMCID: PMC7166204.

100. Kurudenkandy FR, Zilberter M, Biverstal H, Presto J, Honcharenko D, Stromberg R, Johansson J, Winblad B, Fisahn A. Amyloid-beta-induced action potential desynchronization and degradation of hippocampal gamma oscillations is prevented by interference with peptide conformation change and aggregation. J Neurosci. 2014;34(34):11416-25. Epub 2014/08/22. doi: 10.1523/JNEUROSCI.1195-14.2014. PubMed PMID: 25143621.

101. Villette V, Poindessous-Jazat F, Simon A, Lena C, Roullot E, Bellessort B, Epelbaum J, Dutar P, Stephan A. Decreased rhythmic GABAergic septal activity and memory-associated theta oscillations after hippocampal amyloid-beta pathology in the rat. J Neurosci. 2010;30(33):10991-1003. Epub 2010/08/20. doi: 10.1523/JNEUROSCI.6284-09.2010. PubMed PMID: 20720106; PMCID: PMC6633464.

102. Martinez-Losa M, Tracy TE, Ma K, Verret L, Clemente-Perez A, Khan AS, Cobos I, Ho K, Gan L, Mucke L, Alvarez-Dolado M, Palop JJ. Nav1.1-Overexpressing Interneuron Transplants Restore Brain Rhythms and Cognition in a Mouse Model of Alzheimer's Disease. Neuron. 2018;98(1):75-89 e5. Epub 2018/03/20. doi: 10.1016/j.neuron.2018.02.029. PubMed PMID: 29551491; PMCID: PMC5886814.

103. Lambert MP, Barlow AK, Chromy BA, Edwards C, Freed R, Liosatos M, Morgan TE, Rozovsky I, Trommer B, Viola KL, Wals P, Zhang C, Finch CE, Krafft GA, Klein WL. Diffusible, nonfibrillar ligands derived from Abeta1-42 are potent central nervous system neurotoxins. Proc Natl Acad Sci U S A. 1998;95(11):6448-53. PubMed PMID: 9600986; PMCID: PMC27787.

104. McLean CA, Cherny RA, Fraser FW, Fuller SJ, Smith MJ, Beyreuther K, Bush AI, Masters CL. Soluble pool of Abeta amyloid as a determinant of severity of neurodegeneration in Alzheimer's disease. Ann Neurol. 1999;46(6):860-6. PubMed PMID: 10589538.

105. Auld DS, Kar S, Quirion R. Beta-amyloid peptides as direct cholinergic neuromodulators: a missing link? Trends Neurosci. 1998;21(1):43-9. PubMed PMID: 9464686.

106. Lu CB, Li CZ, Li DL, Henderson Z. Nicotine induction of theta frequency oscillations in rodent medial septal diagonal band in vitro. Acta Pharmacol Sin. 2013;34(6):819-29. Epub 2013/03/26. doi: 10.1038/aps.2012.198. PubMed PMID: 23524566; PMCID: PMC4002888.

107. Griguoli M, Cherubini E. Regulation of hippocampal inhibitory circuits by nicotinic acetylcholine receptors. The Journal of physiology. 2012;590(4):655-66. Epub 2011/11/30. doi: 10.1113/jphysiol.2011.220095. PubMed PMID: 22124144; PMCID: PMC3381299.

108. Song C, Murray TA, Kimura R, Wakui M, Ellsworth K, Javedan SP, Marxer-Miller S, Lukas RJ, Wu J. Role of alpha7-nicotinic acetylcholine receptors in tetanic stimulation-induced gamma oscillations in rat hippocampal slices. Neuropharmacology. 2005;48(6):869-80. Epub 2005/04/15. doi: 10.1016/j.neuropharm.2005.01.003. PubMed PMID: 15829257.

109. Alkondon M, Pereira EF, Albuquerque EX. alpha-bungarotoxin- and methyllycaconitine-sensitive nicotinic receptors mediate fast synaptic transmission in interneurons of rat hippocampal slices. Brain research. 1998;810(1-2):257-63. Epub 1998/11/14. doi: 10.1016/s0006-8993(98)00880-4. PubMed PMID: 9813357.

110. Alkondon M, Pereira EF, Albuquerque EX. NMDA and AMPA receptors contribute to the nicotinic cholinergic excitation of CA1 interneurons in the rat hippocampus. Journal of neurophysiology. 2003;90(3):1613-25. Epub 2003/04/19. doi: 10.1152/jn.00214.2003. PubMed PMID: 12702709.

111. Buhler AV, Dunwiddie TV. Regulation of the activity of hippocampal stratum oriens interneurons by alpha7 nicotinic acetylcholine receptors. Neuroscience. 2001;106(1):55-67. Epub 2001/09/21. doi: 10.1016/s0306-4522(01)00257-3. PubMed PMID: 11564416.

112. Buhler AV, Dunwiddie TV. alpha7 nicotinic acetylcholine receptors on GABAergic interneurons evoke dendritic and somatic inhibition of hippocampal neurons. Journal of neurophysiology. 2002;87(1):548-57. Epub 2002/01/11. doi: 10.1152/jn.00316.2001. PubMed PMID: 11784770.

113. Frazier CJ, Buhler AV, Weiner JL, Dunwiddie TV. Synaptic potentials mediated via alpha-bungarotoxin-sensitive nicotinic acetylcholine receptors in rat hippocampal interneurons. J Neurosci. 1998;18(20):8228-35. Epub 1998/10/08. PubMed PMID: 9763468.

114. Lukas RJ, Changeux JP, Le Novere N, Albuquerque EX, Balfour DJ, Berg DK, Bertrand D, Chiappinelli VA, Clarke PB, Collins AC, Dani JA, Grady SR, Kellar KJ, Lindstrom JM, Marks MJ, Quik M, Taylor PW, Wonnacott S. International Union of Pharmacology. XX. Current status of the nomenclature for nicotinic acetylcholine receptors and their subunits. Pharmacological reviews. 1999;51(2):397-401. Epub 1999/06/03. PubMed PMID: 10353988.

115. McClure-Begley TD, King NM, Collins AC, Stitzel JA, Wehner JM, Butt CM. Acetylcholine-stimulated [3H]GABA release from mouse brain synaptosomes is modulated by alpha4beta2 and alpha4alpha5beta2 nicotinic receptor subtypes. Mol Pharmacol. 2009;75(4):918-26. Epub 2009/01/14. doi: 10.1124/mol.108.052274. PubMed PMID: 19139153; PMCID: PMC2684932.

116. Sharma G, Vijayaraghavan S. Modulation of presynaptic store calcium induces release of glutamate and postsynaptic firing. Neuron. 2003;38(6):929-39. Epub 2003/06/24. doi: 10.1016/s0896-6273(03)00322-2. PubMed PMID: 12818178.

117. Sudweeks SN, Yakel JL. Functional and molecular characterization of neuronal nicotinic ACh receptors in rat CA1 hippocampal neurons. The Journal of physiology. 2000;527 Pt 3(Pt 3):515-28. Epub 2000/09/16. doi: 10.1111/j.1469-7793.2000.00515.x. PubMed PMID: 10990538; PMCID: PMC2270092.

118. Frolich L. The cholinergic pathology in Alzheimer's disease--discrepancies between clinical experience and pathophysiological findings. J Neural Transm (Vienna). 2002;109(7-8):1003-13. doi: 10.1007/s007020200083. PubMed PMID: 12111437.

119. Yuede CM, Dong H, Csernansky JG. Anti-dementia drugs and hippocampal-dependent memory in rodents. Behavioural pharmacology. 2007;18(5-6):347-63. Epub 2007/09/01. doi: 10.1097/FBP.0b013e3282da278d. PubMed PMID: 17762506; PMCID: PMC2666934.

120. Vijayraghavan S, Major AJ, Everling S. Muscarinic M1 Receptor Overstimulation Disrupts Working Memory Activity for Rules in Primate Prefrontal Cortex. Neuron. 2018;98(6):1256-68 e4. doi: 10.1016/j.neuron.2018.05.027. PubMed PMID: 29887340.

121. Raina P, Santaguida P, Ismaila A, Patterson C, Cowan D, Levine M, Booker L, Oremus M. Effectiveness of cholinesterase inhibitors and memantine for treating dementia: evidence review for a clinical practice guideline. Ann Intern Med. 2008;148(5):379-97. PubMed PMID: 18316756.

122. Sun Y, Lai MS, Lu CJ, Chen RC. How long can patients with mild or moderate Alzheimer's dementia maintain both the cognition and the therapy of cholinesterase inhibitors: a national population-based study. Eur J Neurol. 2008;15(3):278-83. doi: 10.1111/j.1468-1331.2007.02049.x. PubMed PMID: 18290848.

123. Levin ED, Simon BB. Nicotinic acetylcholine involvement in cognitive function in animals. Psychopharmacology. 1998;138(3-4):217-30. Epub 1998/09/02. PubMed PMID: 9725745.

124. Vicens P, Carrasco MC, Redolat R. Effects of early training and nicotine treatment on the performance of male NMRI mice in the water maze. Neural Plast. 2003;10(4):303-17. Epub 2004/05/22. doi: 10.1155/NP.2003.303. PubMed PMID: 15152984; PMCID: PMC2565429.

125. Buccafusco JJ. Neuronal nicotinic receptor subtypes: defining therapeutic targets. Mol Interv. 2004;4(5):285-95. Epub 2004/10/09. doi: 10.1124/mi.4.5.8. PubMed PMID: 15471911.

126. Hoskin JL, Al-Hasan Y, Sabbagh MN. Nicotinic Acetylcholine Receptor Agonists for the Treatment of Alzheimer's Dementia: An Update. Nicotine Tob Res. 2019;21(3):370-6. Epub 2018/08/24. doi: 10.1093/ntr/nty116. PubMed PMID: 30137524; PMCID: PMC6379052.

127. Bitner RS, Bunnelle WH, Anderson DJ, Briggs CA, Buccafusco J, Curzon P, Decker MW, Frost JM, Gronlien JH, Gubbins E, Li J, Malysz J, Markosyan S, Marsh K, Meyer MD, Nikkel AL, Radek RJ, Robb HM, Timmermann D, Sullivan JP, Gopalakrishnan M. Broad-spectrum efficacy across cognitive domains by alpha7 nicotinic acetylcholine receptor agonism correlates with activation of ERK1/2 and CREB phosphorylation pathways. J Neurosci. 2007;27(39):10578-87. Epub 2007/09/28. doi: 10.1523/JNEUROSCI.2444-07.2007. PubMed PMID: 17898229.

128. Cincotta SL, Yorek MS, Moschak TM, Lewis SR, Rodefer JS. Selective nicotinic acetylcholine receptor agonists: potential therapies for neuropsychiatric disorders with cognitive dysfunction. Curr Opin Investig Drugs. 2008;9(1):47-56. Epub 2008/01/10. PubMed PMID: 18183531.

129. Redrobe JP, Nielsen EO, Christensen JK, Peters D, Timmermann DB, Olsen GM. Alpha7 nicotinic acetylcholine receptor activation ameliorates scopolamine-induced behavioural changes in a modified continuous Y-maze task in mice. European journal of pharmacology. 2009;602(1):58-65. Epub 2008/10/14. doi: 10.1016/j.ejphar.2008.09.035. PubMed PMID: 18848931.

130. Vicens P, Ribes D, Torrente M, Domingo JL. Behavioral effects of PNU-282987, an alpha7 nicotinic receptor agonist, in mice. Behavioural brain research. 2011;216(1):341-8. Epub 2010/08/24. doi: 10.1016/j.bbr.2010.08.015. PubMed PMID: 20728474.

131. Levin ED, Christopher NC. Persistence of nicotinic agonist RJR 2403-induced working memory improvement in rats. Drug Develop Res. 2002;55(2):97-103. doi: 10.1002/ddr.10024. PubMed PMID: WOS:000175328400003.

132. Potasiewicz A, Golebiowska J, Popik P, Nikiforuk A. Procognitive effects of varenicline in the animal model of schizophrenia depend on alpha4beta2- and alpha 7-nicotinic acetylcholine receptors. J Psychopharmacol. 2018;33(1):269881118812097. Epub 2018/12/07. doi: 10.1177/0269881118812097. PubMed PMID: 30501536.

133. Upright NA, Baxter MG. Effects of nicotinic antagonists on working memory performance in young rhesus monkeys. Neurobiology of learning and memory. 2021;184:107505. Epub 2021/08/24. doi: 10.1016/j.nlm.2021.107505. PubMed PMID: 34425219; PMCID: PMC8435017.

134. Sathler MF, Khatri L, Roberts JP, Schmidt IG, Zaytseva A, Kubrusly RCC, Ziff EB, Kim S. Phosphorylation of the AMPA receptor subunit GluA1 regulates clathrin-mediated receptor internalization. Journal of cell science. 2021;134(17). Epub 2021/08/10. doi: 10.1242/jcs.257972. PubMed PMID: 34369573; PMCID: PMC8445600.

135. Sathler MF, Doolittle MJ, Cockrell JA, Nadalin IR, Hofmann F, VandeWoude S, Kim S. HIV and FIV glycoproteins increase cellular tau pathology via cGMP-dependent kinase II activation. Journal of cell science. 2022;135(12). Epub 2022/06/01. doi: 10.1242/jcs.259764. PubMed PMID: 35638570; PMCID: PMC9270957.

136. Lesuisse C, Martin LJ. Long-term culture of mouse cortical neurons as a model for neuronal development, aging, and death. J Neurobiol. 2002;51(1):9-23. Epub 2002/03/29. doi: 10.1002/neu.10037. PubMed PMID: 11920724.

137. Kaech S, Banker G. Culturing hippocampal neurons. Nat Protoc. 2006;1(5):2406-15. Epub 2007/04/05. doi: 10.1038/nprot.2006.356. PubMed PMID: 17406484.

138. Stine WB, Jr., Dahlgren KN, Krafft GA, LaDu MJ. In vitro characterization of conditions for amyloid-beta peptide oligomerization and fibrillogenesis. The Journal of biological chemistry. 2003;278(13):11612-22. doi: 10.1074/jbc.M210207200. PubMed PMID: 12499373.

139. Benson DL, Cohen PA. Activity-independent segregation of excitatory and inhibitory synaptic terminals in cultured hippocampal neurons. J Neurosci. 1996;16(20):6424-32. PubMed PMID: 8815921.

140. Chen TW, Wardill TJ, Sun Y, Pulver SR, Renninger SL, Baohan A, Schreiter ER, Kerr RA, Orger MB, Jayaraman V, Looger LL, Svoboda K, Kim DS. Ultrasensitive fluorescent proteins for imaging neuronal activity. Nature. 2013;499(7458):295-300. Epub 2013/07/23. doi: 10.1038/nature12354. PubMed PMID: 23868258; PMCID: 3777791.

141. Dimidschstein J, Chen Q, Tremblay R, Rogers SL, Saldi GA, Guo L, Xu Q, Liu R, Lu C, Chu J, Grimley JS, Krostag AR, Kaykas A, Avery MC, Rashid MS, Baek M, Jacob AL, Smith GB, Wilson DE, Kosche G, Kruglikov I, Rusielewicz T, Kotak VC, Mowery TM, Anderson SA, Callaway EM, Dasen JS, Fitzpatrick D, Fossati V, Long MA, Noggle S, Reynolds JH, Sanes DH, Rudy B, Feng G, Fishell G. A viral strategy for targeting and manipulating interneurons across vertebrate species. Nat Neurosci. 2016;19(12):1743-9. doi: 10.1038/nn.4430. PubMed PMID: 27798629; PMCID: PMC5348112.

142. Dana H, Sun Y, Mohar B, Hulse BK, Kerlin AM, Hasseman JP, Tsegaye G, Tsang A, Wong A, Patel R, Macklin JJ, Chen Y, Konnerth A, Jayaraman V, Looger LL, Schreiter ER, Svoboda K, Kim DS. High-performance

calcium sensors for imaging activity in neuronal populations and microcompartments. Nature methods. 2019;16(7):649-57. Epub 2019/06/19. doi: 10.1038/s41592-019-0435-6. PubMed PMID: 31209382.

143. Cohen E, Ivenshitz M, Amor-Baroukh V, Greenberger V, Segal M. Determinants of spontaneous activity in networks of cultured hippocampus. Brain research. 2008;1235:21-30. Epub 2008/07/08. doi: 10.1016/j.brainres.2008.06.022. PubMed PMID: 18602907.

144. Kim S, Titcombe RF, Zhang H, Khatri L, Girma HK, Hofmann F, Arancio O, Ziff EB. Network compensation of cyclic GMP-dependent protein kinase II knockout in the hippocampus by Ca2+-permeable AMPA receptors. Proc Natl Acad Sci U S A. 2015;112(10):3122-7. Epub 2015/02/26. doi: 10.1073/pnas.1417498112. PubMed PMID: 25713349; PMCID: 4364185.

145. Kim S, Violette CJ, Ziff EB. Reduction of increased calcineurin activity rescues impaired homeostatic synaptic plasticity in presenilin 1 M146V mutant. Neurobiol Aging. 2015;36(12):3239-46. Epub 2015/10/13. doi: 10.1016/j.neurobiolaging.2015.09.007. PubMed PMID: 26455952; PMCID: 4641803.

146. Kim S, Ziff EB. Calcineurin mediates synaptic scaling via synaptic trafficking of Ca2+-permeable AMPA receptors. PLoS biology. 2014;12(7):e1001900. doi: 10.1371/journal.pbio.1001900. PubMed PMID: 24983627; PMCID: 4077568.

147. Hijioka M, Matsushita H, Ishibashi H, Hisatsune A, Isohama Y, Katsuki H. alpha7 Nicotinic acetylcholine receptor agonist attenuates neuropathological changes associated with intracerebral hemorrhage in mice. Neuroscience. 2012;222:10-9. Epub 2012/07/24. doi: 10.1016/j.neuroscience.2012.07.024. PubMed PMID: 22820264.

148. Bencherif M, Lovette ME, Fowler KW, Arrington S, Reeves L, Caldwell WS, Lippiello PM. RJR-2403: a nicotinic agonist with CNS selectivity I. In vitro characterization. J Pharmacol Exp Ther. 1996;279(3):1413-21. Epub 1996/12/01. PubMed PMID: 8968366.

149. Niimi K, Nishioka C, Miyamoto T, Takahashi E, Miyoshi I, Itakura C, Yamashita T. Improvement of spontaneous alternation behavior deficit by activation of alpha4beta2 nicotinic acetylcholine receptor signaling in the ganglioside GM3-deficient mice. Biomed Res. 2013;34(4):189-95. Epub 2013/09/03. doi: 10.2220/biomedres.34.189. PubMed PMID: 23995055.

150. Duris K, Manaenko A, Suzuki H, Rolland WB, Krafft PR, Zhang JH. alpha7 nicotinic acetylcholine receptor agonist PNU-282987 attenuates early brain injury in a perforation model of subarachnoid hemorrhage in rats.

Stroke; a journal of cerebral circulation. 2011;42(12):3530-6. Epub 2011/10/01. doi: 10.1161/STROKEAHA.111.619965. PubMed PMID: 21960575; PMCID: PMC3226904.

151. Kawamura N, Novianti E, Yamada-Goto N, Nakama R, Asakawa A, Katsuura G, Inui A. Activation of alpha7 nicotinic receptors suppresses sucrose addiction in mice. Progress in neuro-psychopharmacology & biological psychiatry. 2022;113:110439. Epub 2021/09/14. doi: 10.1016/j.pnpbp.2021.110439. PubMed PMID: 34517054.

152. Hajos M, Hurst RS, Hoffmann WE, Krause M, Wall TM, Higdon NR, Groppi VE. The selective alpha7 nicotinic acetylcholine receptor agonist PNU-282987 [N-[(3R)-1-Azabicyclo[2.2.2]oct-3-yl]-4-chlorobenzamide hydrochloride] enhances GABAergic synaptic activity in brain slices and restores auditory gating deficits in anesthetized rats. J Pharmacol Exp Ther. 2005;312(3):1213-22. Epub 2004/11/04. doi: 10.1124/jpet.104.076968. PubMed PMID: 15523001.

153. Smith AD, Dar MS. Behavioral cross-tolerance between repeated intracerebellar nicotine and acute Delta(9)-tetrahydrocannabinol-induced cerebellar ataxia: role of cerebellar nitric oxide. J Pharmacol Exp Ther. 2007;322(1):243-53. Epub 2007/04/10. doi: 10.1124/jpet.107.120634. PubMed PMID: 17416741.

154. Lippiello PM, Bencherif M, Gray JA, Peters S, Grigoryan G, Hodges H, Collins AC. RJR-2403: a nicotinic agonist with CNS selectivity II. In vivo characterization. J Pharmacol Exp Ther. 1996;279(3):1422-9. Epub 1996/12/01. PubMed PMID: 8968367.

155. Sapronov NS, Fedotova YO, Kuznetsova NN. Antiamnestic effect of alpha7-nicotinic receptor agonist RJR-2403 in middle-aged ovariectomized rats with Alzheimer type dementia. Bull Exp Biol Med. 2006;142(6):700-2. Epub 2007/07/03. doi: 10.1007/s10517-006-0455-y. PubMed PMID: 17603674.

156. Siegle JH, Lopez AC, Patel YA, Abramov K, Ohayon S, Voigts J. Open Ephys: an open-source, plugin-based platform for multichannel electrophysiology. J Neural Eng. 2017;14(4):045003. Epub 2017/02/09. doi: 10.1088/1741-2552/aa5eea. PubMed PMID: 28169219.

157. Tadel F, Baillet S, Mosher JC, Pantazis D, Leahy RM. Brainstorm: A User-Friendly Application for MEG/EEG Analysis. Computational Intelligence and Neuroscience. 2011;2011(1):879716. doi: https://doi.org/10.1155/2011/879716.

158. Klug M, Berg T, Gramann K. Optimizing EEG ICA decomposition with data cleaning in stationary and mobile experiments. Sci Rep. 2024;14(1):14119. Epub 20240619. doi: 10.1038/s41598-024-64919-3. PubMed PMID: 38898069; PMCID: PMC11187149.

Figure 1. Nicotinic cholinergic regulation of cultured hippocampal PV+ and SST+ interneurons is mainly mediated by α7- and α4β2-nAChRs, respectively.

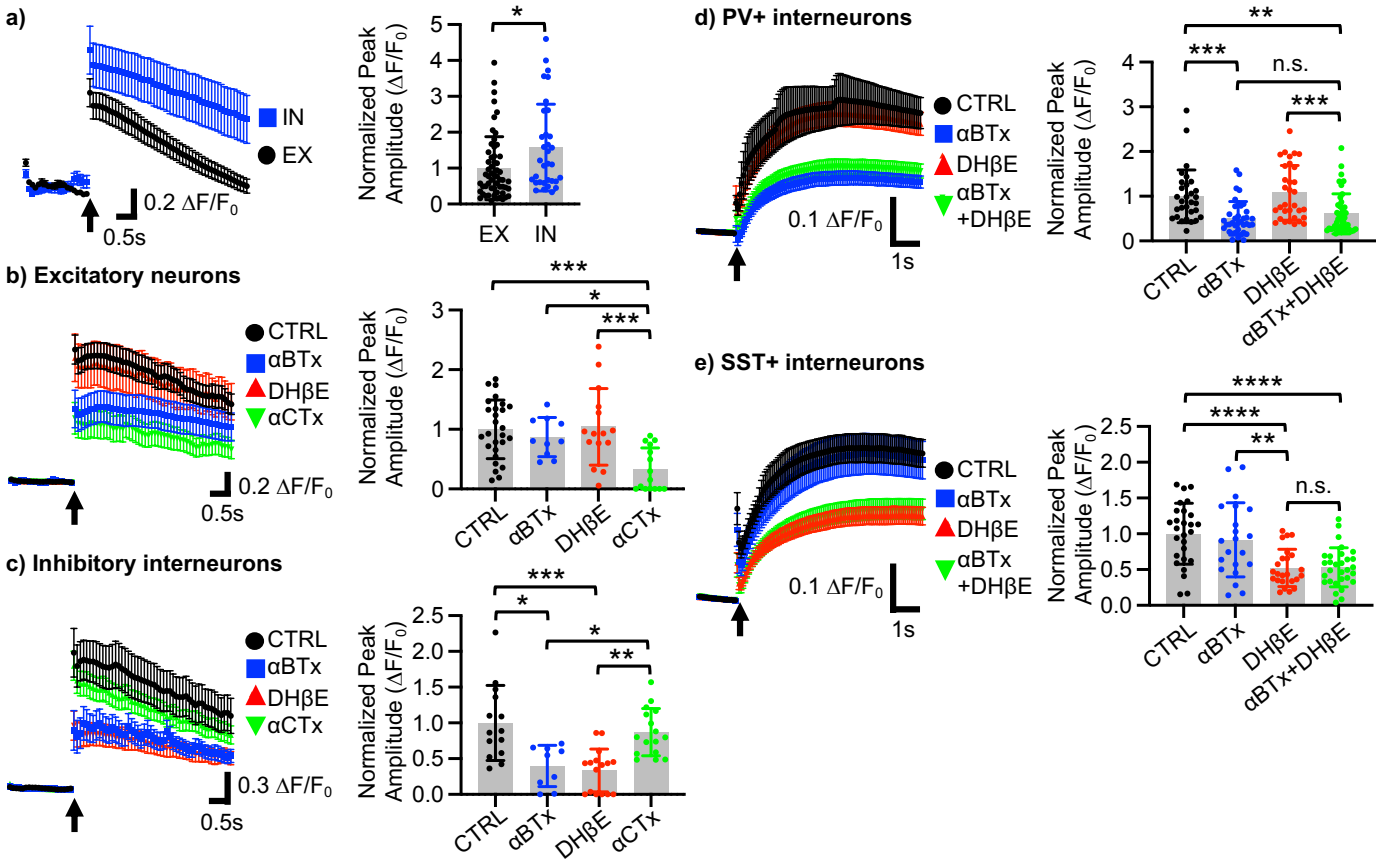

a) Average traces of GCaMP6f signals in excitatory (EX) and inhibitory (IN) cells and summary data of normalized peak amplitude in each condition (n = number of cells excitatory cells = 57 and inhibitory cells =33 from 4 pups in 2 independent cultures). *$p < 0.05$, two-tailed student's t-test. Average traces of GCaMP6f signals and summary graphs of normalized peak amplitude in each condition in **b)** excitatory (n = number of cells, CTRL = 27, αBTx = 10, DhβE = 15, and αCTx = 15 from 4 pups in 2 independent cultures) and **c)** inhibitory cells (n = number of cells, CTRL = 14, αBTx = 9, DhβE = 16, and αCTx = 16 from 4 pups in 2 independent cultures). Average traces of GCaMP7s signals and summary data of normalized peak amplitude in each condition in **d)** PV+ (n = number of cells, CTRL = 30, αBTx = 38, DhβE = 32, and αBTx+DhβE =43 from 6 pups in 3 independent cultures) and **e)** SST+ cells (n = number of cells, CTRL = 27, αBTx = 21, DhβE = 24, and αBTx+DhβE = 30 from 6 pups in 3 independent cultures). *$p < 0.05$, **$p < 0.01$, ***$p < 0.001$, and ****$p < 0.0001$. one-way ANOVA, Tukey test. An arrow indicates photostimulation. n.s.: not significant.

Figure 2. The Aβ-induced decrease in the neuronal activity of PV+ and SST+ interneurons is reversed by stimulation of α7- and α4β2-nAChRs, respectively.

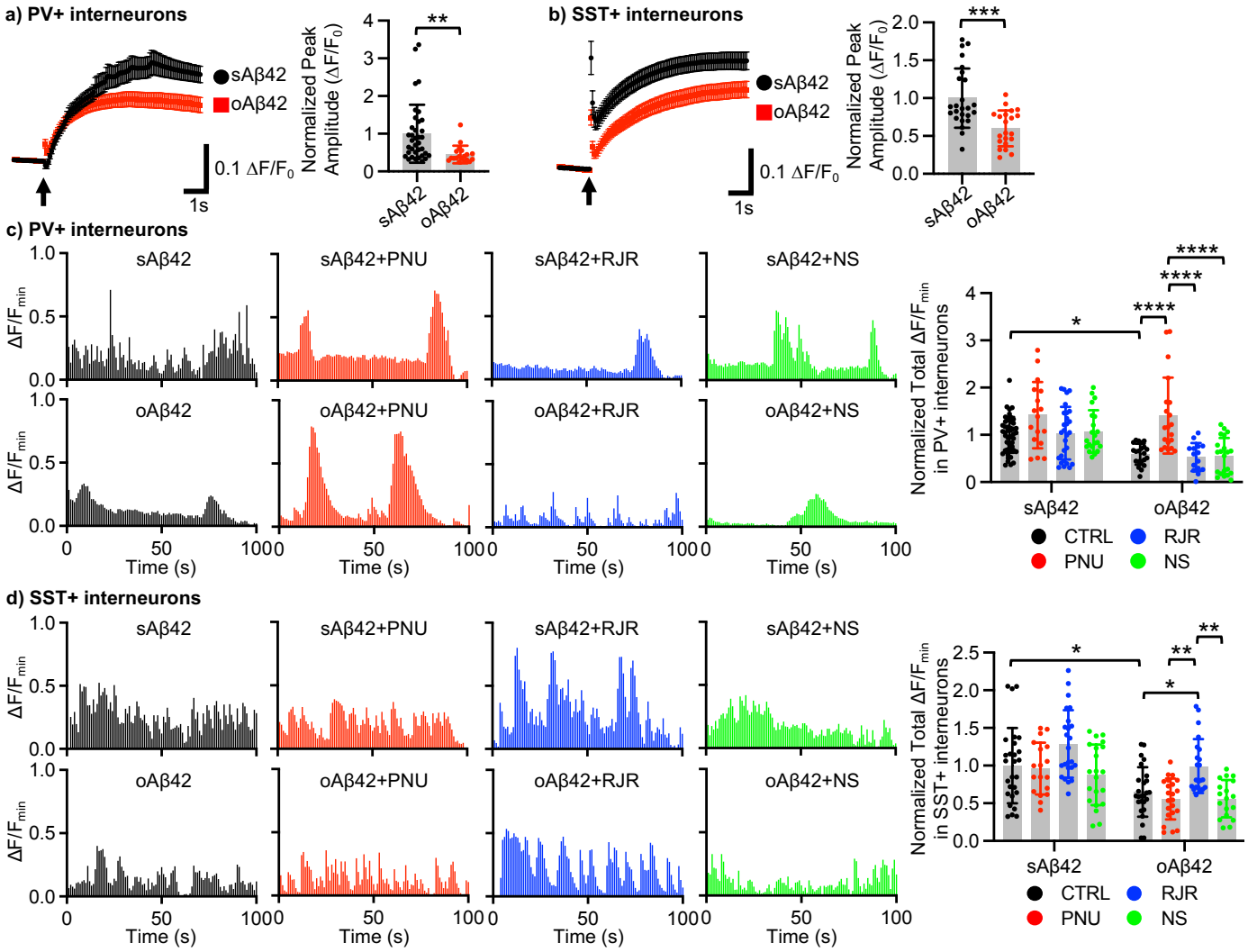

Average traces of GCaMP7s signals and summary data of normalized peak amplitude in each condition in **a)** PV+ cells (n = number of cells, sAβ42 = 36 and oAβ42 = 19 from 6 pups in 3 independent cultures) and **b)** SST+ cells (n = number of cells, sAβ42 = 25 and oAβ42 = 21 from 6 pups in 3 independent cultures). $^{**}p < 0.01$ and $^{***}p < 0.001$, two-tailed student's t-test. An arrow indicates photostimulation. Representative traces of GCaMP7s fluorescence intensity and summary graphs of normalized total Ca^{2+} activity in each condition in **c)** PV+ (n = number of cells, sAβ42:CTRL = 47, sAβ42:PNU = 17, sAβ42:RJR = 28, sAβ42:NS = 21, oAβ42:CTRL = 21, oAβ42:PNU = 20, oAβ42:RJR = 15, and oAβ42:NS = 21 from 6 pups in 3 independent cultures) and **d)** SST+ interneurons (n = number of cells, sAβ42:CTRL = 27, sAβ42:PNU = 18, sAβ42:RJR = 24, sAβ42:NS = 21, oAβ42:CTRL = 26, oAβ42:PNU = 22, oAβ42:RJR = 22, and oAβ42:NS = 18 from 6 pups in 3 independent cultures). $^{*}p < 0.05$, $^{**}p < 0.01$, and $^{****}p < 0.0001$, Two-way ANOVA, Tukey test.

Figure 3. Deficits in hippocampal network activity in 5XFAD mice following fear learning.

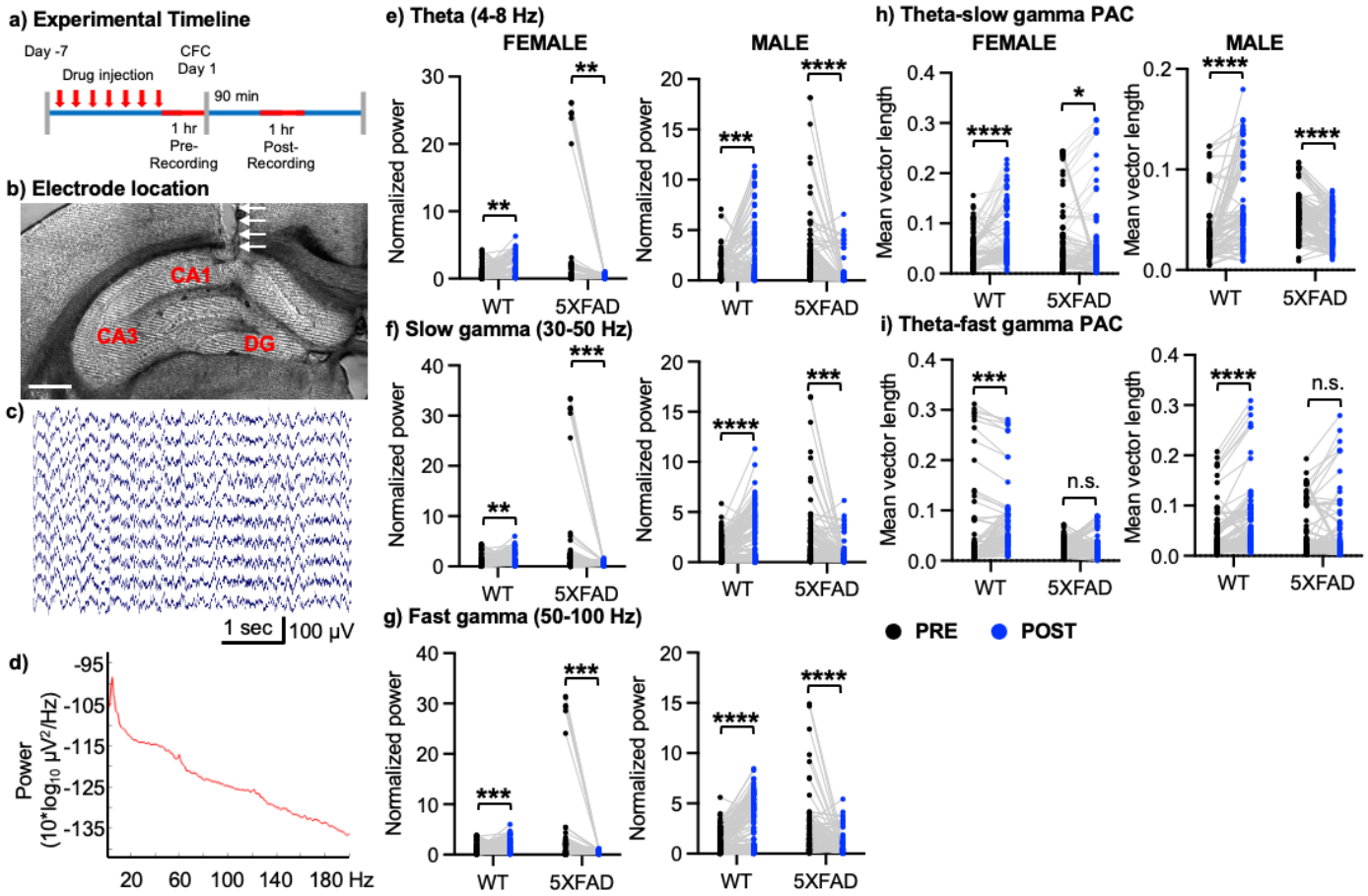

a) Experimental timeline. **b)** A representative image of a brain section after electrolytic lesioning indicates electrode placement (arrows) in the hippocampus CA1 area. A scale bar represents 1 mm. **c)** Representative section of LFP traces in CA1 of a freely behaving mouse. **d)** Representative power spectral density. Summary graphs of normalized powers of **e)** theta, **f)** slow gamma and **g)** fast gamma frequencies in female and male mice in each condition (Two-Way ANOVA, Two-stage linear step-up procedure of Benjamini, Krieger and Yekutieli test). Summary of **h)** Theta-slow gamma PAC and **i)** Theta-fast gamma PAC in each condition (Paired two-tailed Student's t-test). n = number of channels [number of animals]; Female, WT =74 [7] and 5XFAD = 101 [9], Male, WT =125 [12] and 5XFAD = 108 [10]). *$p < 0.05$, **$p < 0.01$, ***$p < 0.001$, and ****$p < 0.0001$. n.s. – not significant.

Figure 4. Co-activation of α7- and α4β2-nAChRs is required to restore normal hippocampal network activity in 5XFAD mice.

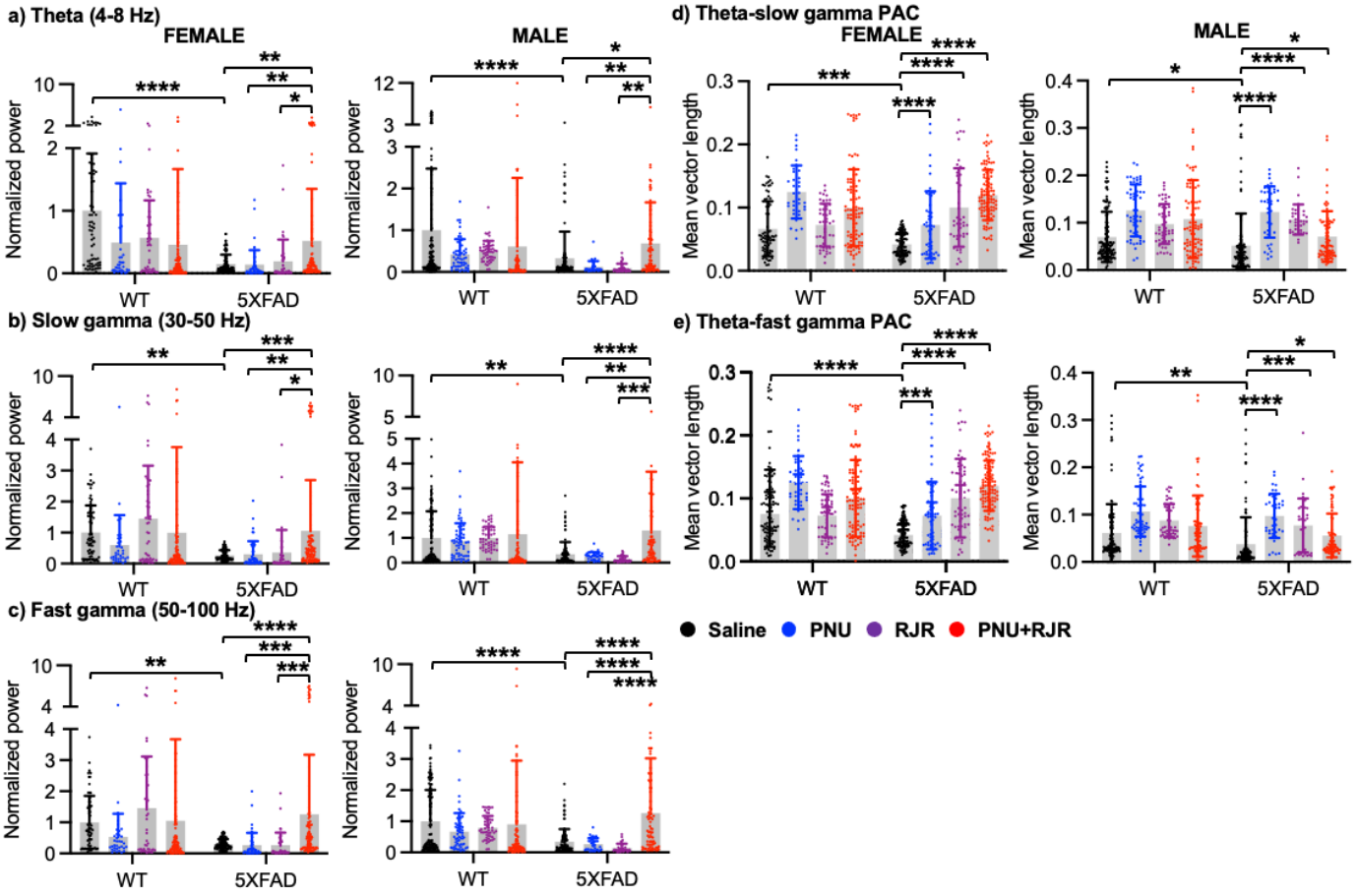

Summary graphs of normalized powers of **a)** theta, **b)** slow gamma and **c)** fast gamma frequencies in female and male mice in each condition (Two-Way ANOVA, Two-stage linear step-up procedure of Benjamini, Krieger and Yekutieli test). Summary of **d)** Theta-slow gamma PAC and **e)** Theta-fast gamma PAC in each condition (Paired two-tailed Student's t-test). n = number of channels [number of animals]; Female, WT:Saline =74 [7], WT:PNU = 49 [4], WT:RJR = 48 [4], WT:PNU+RJR = 97 [9], 5XFAD:saline = 101 [9], 5XFAD:PNU = 51 [4], 5XFAD:RJR = 43 [4], and 5XFAD:PNU+RJR = 93 [8], Male, WT:Saline =125 [12], WT:PNU = 57 [5], WT:RJR = 51 [4], WT:PNU+RJR = 86 [8], 5XFAD:saline = 108 [10], 5XFAD:PNU = 36 [4], 5XFAD:RJR = 38 [4], and 5XFAD:PNU+RJR = 79 [7]. *$p < 0.05$, **$p < 0.01$, ***$p < 0.001$, and ****$p < 0.0001$.

Figure 5. Co-activation of α7- and α4β2-nAChRs is required to improve contextual fear memory in 5XFAD mice.

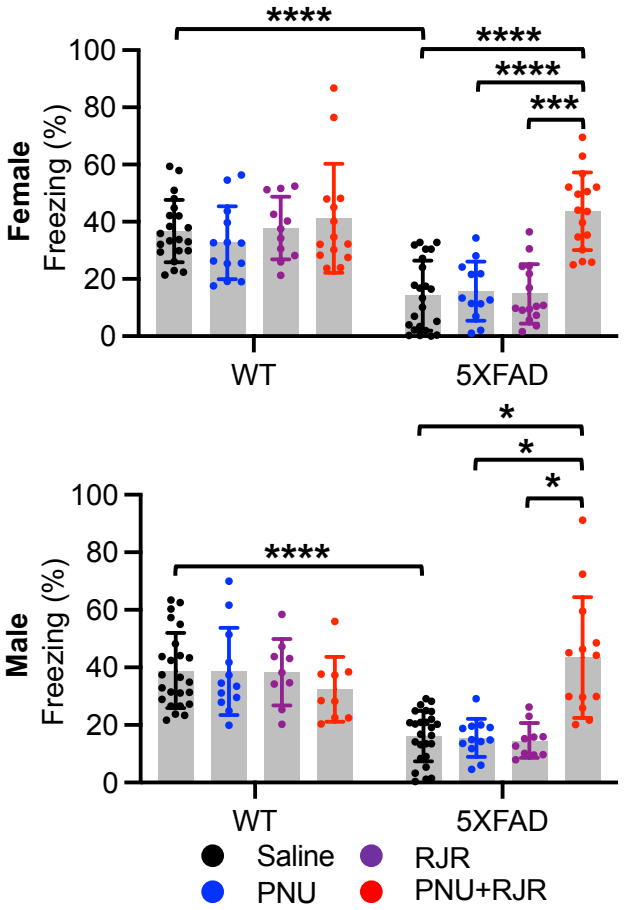

Summary data of freezing behavior of WT and 5XFAD female (n = number of animals, WT:Saline = 21, WT:PNU = 13, WT:RJR = 11, WT:PNU+RJR = 14, 5XFAD:Saline = 23, 5XFAD:PNU = 12, 5XFAD:RJR = 15, 5XFAD:PNU+RJR = 16) and male mice (n = number of animals, WT:Saline = 24, WT:PNU = 12, WT:RJR = 9, WT:PNU+RJR = 9, 5XFAD:Saline = 26, 5XFAD:PNU = 12, 5XFAD:RJR = 10, 5XFAD:PNU+RJR = 13) in each condition. *$p < 0.05$ and ****$p<0.0001$, Two-way ANOVA, Tukey test.

Figure 6. A schematic model of nAChR-mediated mechanisms of Aβ-induced dysfunction in hippocampal inhibition, network activities, and memory in AD.

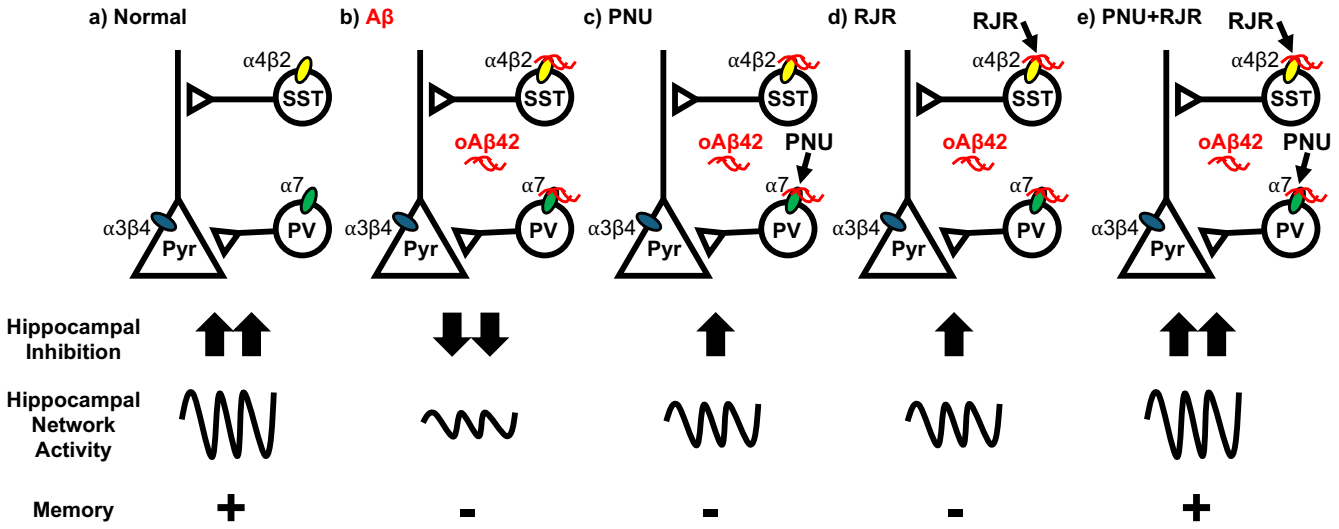

a) A simplified local inhibitory circuit in the hippocampus. PV+ interneurons mainly provide somatic inhibition to pyramidal excitatory neurons (Pyr), while SST+ interneurons provide dendritic inhibition. This contributes to hippocampal oscillations and cognitive function. α7-, α4β2-, and α3β4-nAChRs predominantly control nicotinic cholinergic signaling in PV-, SST-, and pyramidal cells, respectively. **b)** Aβ selectively inhibits α7- and α4β2-nAChRs in inhibitory cells, but not α3β4-nAChRs, in turn reduces inhibitory inputs to excitatory cells, which contributes to disruptions in hippocampal oscillations and consequent learning and memory in AD. **c-d)** Single stimulation of each nAChR subtype by PNU-282987 (PNU), an α7 agonist, or RJR-2403 Oxalate (RJR), an α4β2 agonist, is unable to reverse the Aβ-induced adverse effects on network activity and memory. **e)** Co-stimulation of α7- and α4β2-nAChRs sufficiently restores normal hippocampal oscillations and memory.